SAC200164730000

SECRET RD

UNCLASSIFIED

UCRL 53880-3-2

~~This document consists of 118 pages.~~
No. 616 ~~of 720 copies. Series A.~~

29 pgs

DEFENSE RESEARCH REVIEW (U)

VOLUME 3 July 1991 NUMBER 2

LOS ALAMOS
01912663

UCRL-53880-3-2 616A
19-FEB-92 11:50 OA 1343 LOS ALAMOS NATIONAL LAB

Published by

LOS ALAMOS NATIONAL LABORATORY

LAWRENCE LIVERMORE NATIONAL LABORATORY

SANDIA NATIONAL LABORATORIES

DEPARTMENT OF ENERGY DECLASSIFICATION REVIEW

1st REVIEW-DATE: 6/25/02
AUTHORITY: ☐ OC ☒ DD
NAME: Mel Lewis

2nd REVIEW-DATE: 8/10/2001
AUTHORITY: DD
NAME: Phil Lang, ADD

DETERMINATION [CIRCLE NUMBER(S)]
1. CLASSIFICATION RETAINED
2. CLASSIFICATION CHANGED TO:
3. CONTAINS NO DOE CLASSIFIED INFO
4. COORDINATE WITH:
5. CLASSIFICATION CANCELED:
6. CLASSIFIED INFO BRACKETED
7. OTHER (SPECIFY):

DERIVATIVE CLASSIFIER
Roger M. White
Senior Scientific Editor
Defense Research Review
Physics Department, LLNL

RESTRICTED DATA. This document contains Restricted Data as defined in the Atomic Energy Act of 1954. Unauthorized disclosure subject to Administrative and Criminal Sanctions.

CRITICAL NUCLEAR WEAPON DESIGN INFORMATION. DoD DIRECTIVE 5210 APPLIES.

NUCLEAR WEAPON DATA. Sigma 1

SECRET RD

UNCLASSIFIED

01SA20C000132

SECRET RD
SAC20016473000

Defense Research Review VOLUME 3, NUMBER 2 July 1991

UNCLASSIFIED

THE ICF GAIN CURVE: A PREDICTION BASED ON CURRENT TARGET PHYSICS DATA (U)

W. C. Mead, B. Bezzerides, S. V. Coggeshall, M. Cray,
H. N. Fisher, N. M. Hoffman, and G. R. Magelssen
Los Alamos National Laboratory, Los Alamos, NM 87545

(Received May 1990; revised May 1991)

We present our current predictions for the gain of hydrodynamically-scaled, indirect-drive, inertial-confinement-fusion (ICF) targets. We discuss the formulation of gain curves and some key physical processes that enter the predictions. To predict the performance of future ICF targets, we have constructed a scaling model that contains a few of the most basic features of ICF target operation and parametrizes the possible effects of other complex target processes. We assessed the values and uncertainties of the model parameters through detailed calculations and estimates of the underlying target physics processes and extrapolations of current data. We present Monte Carlo calculations that determine the propagation of the estimated uncertainties to the "high-gain ICF" regime. We find that remaining target physics and design issues lead to large uncertainties in target gain predictions. We discuss present and (hypothetical) future experimental constraints on the theoretical models and discuss the resulting gain predictions and uncertainties. (SRD)

I. INTRODUCTION

For some applications of inertial confinement fusion (ICF), the target gain curve represents the "bottom line" for predicting target performance. We are interested in determining the minimum driver requirements for achieving gain in the laboratory. As the field of ICF has matured, more and more details are known about the underlying physical processes that determine the gain curve, and larger amounts of relevant data exist. In this paper we present a new methodology developed for combining the relevant information from many sources, and we determine, based on current knowledge, the location and uncertainty in the target gain curve.

In order to understand the uncertainties involved in predicting the performance of future ICF targets, we have constructed a model that contains a few of the most basic features of ICF target operation and mocks up the possible effects of other complex target processes via simple parametrizations. In the interest of simplicity and accuracy, the gain curve model is a framework that can incorporate state-of-the-art knowledge from a variety of sources. A schematic of the model is shown in Fig. 1. Throughout this work we use "target" to denote a spherical, thermonuclear "capsule" driven by x-rays contained in a laser-heated "hohlraum." The target gain is factored into a capsule gain and an overall hohlraum efficiency. Definitions of the capsule and target gain, and of the hohlraum coupling efficiency are as shown. We assumed that the hohlraum would be optimized to meet the capsule drive requirements with negligible capsule degradation. That is, the hohlraum will incur whatever efficiency penalty is necessary to meet the drive requirements of a highly optimized hydrodynamically-scaled capsule (HSC). We note that different target design approaches are possible that trade off capsule performance against improved hohlraum efficiency and that these options remain to be explored.

For this entire study, we focus our attention on hydrodynamically-scaled targets (HSTs). We define the HST both conceptually and more technically. Conceptually, an HST is an ICF single-shell, radiation-driven capsule (the HSC) plus the hohlraum that converts laser light into drive x-rays. The HSC is a capsule design class that operates in a particular qualitative mode: the HSC, when hydrodynamically scaled to typical ICF drive energies (say, 3–10 MJ), must ignite and produce high gain. More technically, an HST, as used here, is a single-shell, low-Z, precision-pulse-shaped capsule, imploded spherically to obtain a central hot spot (sometimes called an "ignitor") and a low-entropy main fuel and pusher region,[1,2] together with the hohlraum[3] that provides the drive x-rays to the capsule with the spectrum, time dependence, and symmetry required to achieve optimum capsule performance. When referring to just the scaled capsule, we denote it as HSC. Most of the HSC design

SECRET RD
UNCLASSIFIED

UNCLASSIFIED SECRET/RD

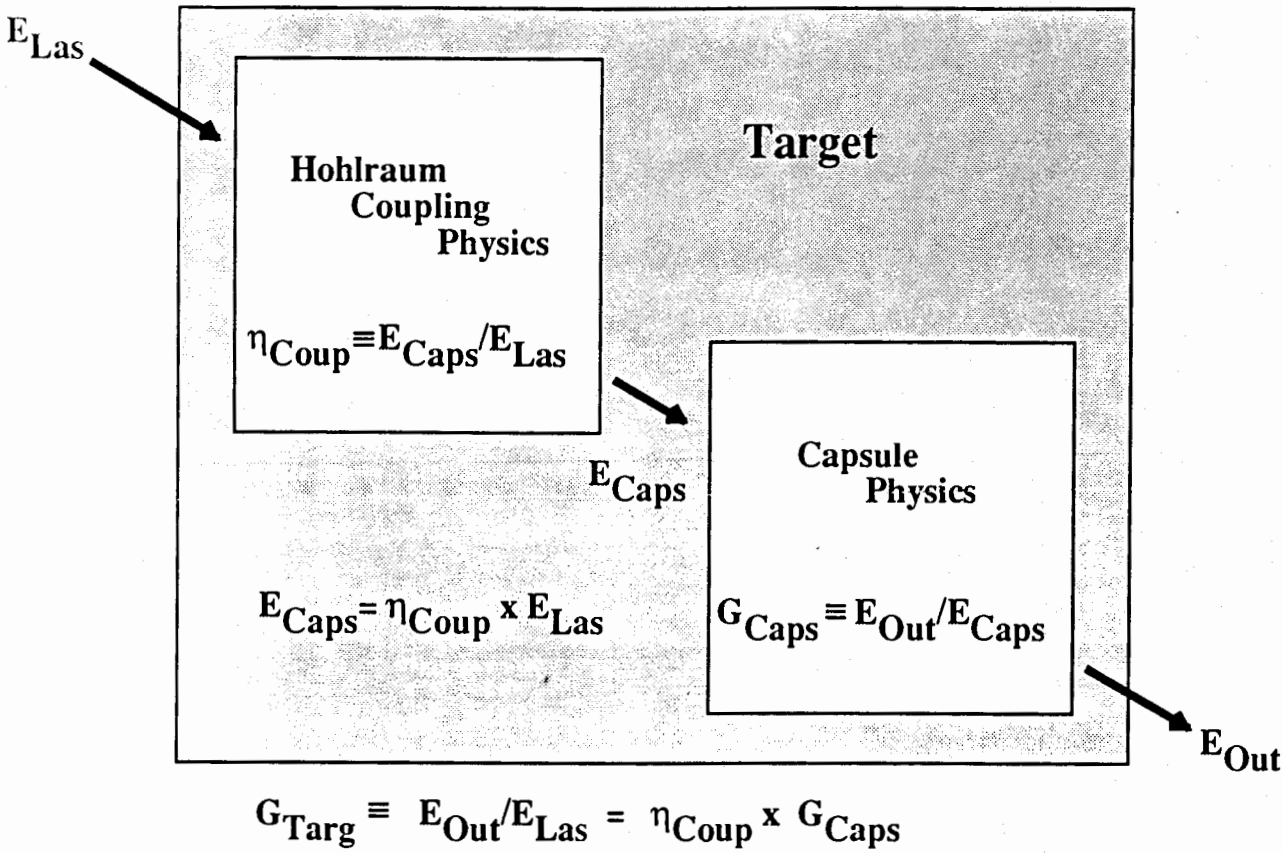

Fig. 1. Performance of an ICF indirect-drive target can be factored into two major blocks.

calculations presented here assume a foam/cryogenic-DT ablator/pusher with cryogenic DT fuel. A few HSC designs with beryllium ablators and cryogenic DT fuel were tried, and these showed performance and behavior similar to the foam designs.

Perhaps a brief historical digression will help to explain the value of the HST concept. Early ICF target experiments were performed using simple targets that shock and preheat the DT fuel to high entropy. The capsules that operate most clearly in this mode are called "exploding pushers." Typically, the fuel in such capsules is driven to pressures (at a given density) that exceed the Fermi degenerate value by a factor of 100 or more. Recently, so-called "intermediate density" and "high density" targets use somewhat modified capsule designs and pulse shapes to achieve what might be called "swelling-pusher" implosions, compressing the fuel at pressures of 10 to 30 times degenerate. None of these (non-HSC) capsule types scales hydrodynamically to achieve high gain at a reasonable laboratory driver energy, since the energy required to compress high-entropy DT is too great.

Prior to this work, and partly for historical, programmatic reasons, gain curves and data collections mixed these various target types. At the lowest driver energies, exploding pusher data points were plotted, since this capsule type takes advantage of high fuel temperatures to achieve relatively high yields (though low gains) without stringent driver requirements. As the program progressed to the higher drive energies of Livermore's Argus, Shiva, and Nova lasers, target designs and experiments shifted to intermediate- and high-density targets, so these data were plotted. At higher energies, which are considered goals for laboratory-driven high-gain ICF, predictions were plotted for the high-gain designs, including the class referred to here as HSTs.

[redacted] b(3)

SECRET/RD
UNCLASSIFIED

UNCLASSIFIED SECRET/RD

b(3)

We have refined an old concept (due to J. Lindl and J. Nuckolls, ca. 1975), the "Hydrodynamically Equivalent Target," and invented a name that accurately describes the restricted class of targets and capsules we define. Thus, we arrived at the conceptual definition given above. Now, we plot a new, more qualitatively consistent gain curve that represents the single target class called HSTs. When we include non-HST data points, we explicitly so note, and we plot our best estimates of the implications of those data for HSTs. The low and high ends of this scaling curve can then presumably be investigated on the basis of existing or future data. This somewhat reduces the problem of interpolation, making the process more quantitative rather than qualitative.

Another way of viewing this process is that we wish to separate issues associated with qualitative operating modes from quantitative scaling issues. This should permit predictions, interpolations, and extrapolations to be made in a conceptually-clearer framework. It should also permit evaluation of near-term experiments to determine more clearly their impact on future high-gain ICF targets. These are the conceptual advantages of the HST/HSC concept.

We close the historical perspective with a note intended to avoid conceptual traps for the future. It is possible, because of the quantitative scaling issues, that low- and high-energy HSTs might behave differently just because some of the target or capsule physical processes have scaled through different regimes. Thus, in spite of narrowing the class to qualitatively-similar, hydrodynamically-scaled designs, it is still possible that low-energy HSTs could fail while high-energy HSTs could work more-or-less as calculated, or vice versa. Thus, it remains a matter of great importance to maintain a clear conceptual and physical understanding of the scalings and underlying physical processes involved. Until a high-gain ICF target is fully tested and proven, data and scaling knowledge alone cannot completely replace detailed target physics understanding.

The ICF target physics data base is diverse and has varying relevance to predicting the performance of HSTs. We have handled this diversity by using the information available in a hierarchically-weighted scheme, as indicated in Fig. 2. Actual optimized-HST data points would be relied on most heavily.

b(

Thus, extrapolated data are next in weight and represent the most heavily-weighted feature of available data. We considered the experimental and analysis uncertainties and the qualitative and quantitative features of the extrapolation to determine an effective uncertainty in predictions at optimum HST conditions. At the next lower priority are clean-1D (no-mix) LASNEX[4] calculations, followed by calculations using developmental models. LASNEX calculations have an implicit but important role in the entire process by providing the prototype of an HST, which serves as a conceptual goal and yardstick for evaluating the relevance of all data. Extrapolations of data to HST conditions are also evaluated based upon LASNEX calculations performed to analyze the experimental data. Inevitably, we must invoke intuition and judgment to meld available information and to make up for missing information. The framework developed here makes such exertions of judgment obvious, in effect self-consistently quantifying the impact of missing knowledge on the gain curve. Because of the necessity to exercise considerable judgment, much of the discussion below is more properly thought as a rationale rather than a closed-form calculation of the gain curve. We have presented a number (though not all) of the back-of-the-envelope estimates that are necessary to supply knowledge not available from other sources. These are obviously uncertain, but are included to lend some plausibility to the gain curve

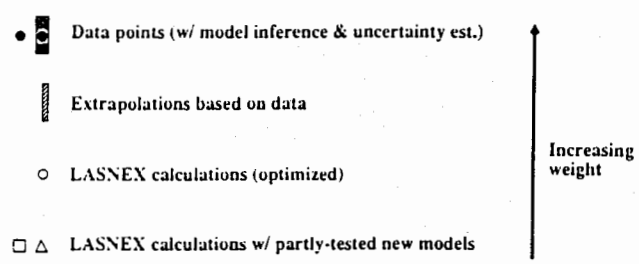

Fig. 2. "Realistic" gain curve includes most-relevant parts of the current ICF target physics data base.

UNCLASSIFIED SECRET/RD

UNCLASSIFIED SECRET/RD

estimates and the scenarios that might be possible. In the most uncertain physics areas, we estimate plausible upper and lower cases and use these to define the current predictive uncertainty.

Each section of the model is constructed with appropriate scaling functions and parameters. The functional dependences of the different model sections, or sub-models, are chosen to represent, approximately, our expectations for the scaling of the particular physical process(es) involved, based on current theoretical and experimental knowledge. As will be seen shortly, we believe the actual uncertainties in the data base exceed any uncertainties introduced by exact, assumed details of the probability and scaling functions. We input median values for the parameters, based on our best application of the current target physics data base. We assume, for lack of better knowledge, that each of the model parameters is uncertain about its median value by a multiplicative or additive value that has a gaussian probability distribution function, and choose the uncertainty for each model parameter to satisfy the constraints we can generate from the target physics data base. We chose the gaussian form for the probability distribution functions based on the Central Limit Theorem and our assessment that these parameters are determined by a system having many degrees of freedom. We then use Monte Carlo techniques to select random combinations of the model parameters, treating the outcome as a "universe" of possible outcomes. Statistical summaries of the possible outcomes allow us to make quantitative statements of the likelihood of various interesting outcomes. By imposing constraints based on the (hypothetical) results of (possible) future experiments, we can quantitatively examine the impact of such experiments on the position and uncertainty of different portions of the gain curve.

By the assumptions and design of our model for gain prediction, its meaning is somewhat different from other ICF gain predictions used in previous[5] and other contemporary[6] work. Most ICF gain curves are based primarily on design calculations using the best models available. The calculations usually assume that certain potentially-limiting physics issues can be successfully resolved. Such issues are sometimes presented as ancillary caveats to the gain curve or are folded into the gain curve through "derating" factors determined by some rationale. This approach has value for some kinds of planning. However, in the present work we have chosen to be as comprehensive as possible, including all known and potentially-significant target physics processes explicitly. Currently-available experimental results have been weighted heavily and have been extrapolated to the conditions of our best predictions of high-gain ICF targets. We have not included target design or physics "learning"; i.e., we have not explicitly included target refinements that are currently unknown. Thus, our gain predictions are "current" and do not necessarily represent limits on what can be achieved in the future with greater design and physics sophistication, or perhaps breakthroughs. There are at least three benefits of our present approach: (1) the assumptions made are visible and explicit; (2) we have a comprehensive, definite, fairly quantitative predictive tool, encompassing all current target physics knowledge; and (3) as future refinements of knowledge and design are made, the framework developed here will allow quantitative assessment and demonstration of the progress.

This paper is organized to parallel the main sections of the model. In the following sections, we discuss the model inputs in each major physics area, then present and discuss global model results.

II. CAPSULE GAIN

The capsule gain model is a parametrization of the basic operating characteristics of an ICF capsule. As indicated in Fig. 3, capsule performance has three regimes: (1) pre-ignition (low gain); (2) bootstrapping; and (3) high gain. The six adjustable parameters of the capsule gain model (see Appendix A), are chosen to satisfy constraints provided by the available capsule physics data base. The data base for capsule physics and performance is shown in Fig. 4.

[redacted] b(3)

Next we discuss the specifics of these data base elements, in turn.

A. Centurion/Halite and Nova data

[redacted] b(3)

SECRET/RD UNCLASSIFIED

SECRET/RD

UNCLASSIFIED

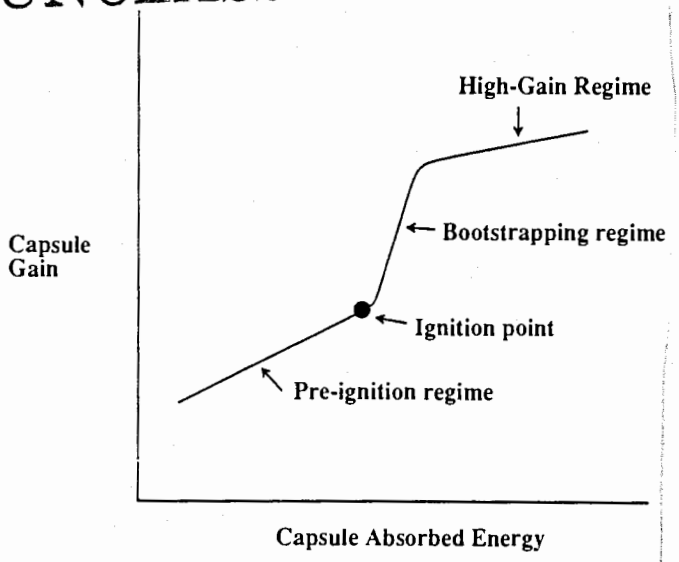

Fig. 3. Capsule gain model has basic causality and parametrizes capsule operating regimes.

b(3)

b(3)

The Nova capsule data point[8] corresponds to a medium-convergence, DT-gas-filled, glass-pushered capsule. The glass pusher (ρ = 2.2 g/cm^3) was 9 μm thick with an inside diameter of 360 μm. The pusher was coated with a 32-μm-thick layer of CH (ρ = 1 g/cm^3). The DT gas fill was 50 atmospheres (ρ = 0.01 g/cm^3).

SECRET/RD
UNCLASSIFIED

UNCLASSIFIED SECRET/RD

Several tests of this capsule were performed during 1986–87 in standard "1.0-scale" Nova hohlraums, using flat-topped, 1-ns pulses (100 ps rise and fall times), at about 18 kJ total laser energy. Hohlraum conditions for these tests are discussed below. We (and LLNL[8]) estimate from LASNEX calculations that the capsule absorbed about 1.7 ± 0.4 kJ of x-ray drive energy. The measured yields[8] from capsules of this configuration were about 4×10^{10} DT neutrons, with a scatter of plus or minus a factor of about 3. This gives a capsule gain of about 8×10^{-5}.

The calculated and observed convergence ratio[8] for this Nova capsule under these drive conditions is about 9. Our calculations predict that the implosion history for this capsule shows strong shock preheating of the pusher and fuel, followed by pusher decompression throughout much of the implosion, then recompression to achieve fuel densities of about 5–10 g/cm^3.

b(3) [redacted] Depending upon the details of the LASNEX model used to analyze this target's performance, the yield observed over calculated yield (YOC) is in the range of 0.1–1. The qualitative nature of this implosion is, of course, very different from that of an HSC.

B. Extrapolations of data to HSC conditions

An area of judgment arises in extrapolating the capsule data to HSC conditions. How much performance improvement (or degradation?) should be expected? How much uncertainty is entailed in the extrapolation? Two approaches to answering these questions were considered.

b(3) [redacted] On this basis alone, we can argue that predictions for *any capsule of comparable physics and design sensitivity* are best made from optimized calculations by assuming YOC = 0.5 and taking an uncertainty in gain of plus or minus about a factor of 2. Similar predictive uncertainties and degradations are seen in analyzing the results of low-to-moderate-convergence Nova implosion experiments.[9] (Note, however, that Nova capsule experiments show a strong trend toward poorer-than-calculated performance as the convergence ratio increases, probably as a result of asymmetric drive and/or mix.)

b(3) [redacted] This suggests that a reasonable (but possibly optimistic) first cut at performance and uncertainty predictions for HSCs would be to assume YOC = 0.5 plus or minus a factor of 2.

Second, to refine this estimate, we considered the question, "What is specifically entailed in extrapolating from recently-tested capsules to the HSC regime, and what risks or unknowns are involved in the extrapolation?" The nature of the extrapolation is toward a regime with (1) greater entropy difference between hot-spot and main fuel, (2) lower entropy in the main fuel and pusher, (3) greater dynamic range and precision of pulse shaping, (4) generally higher convergence ratio (CR), and (5) somewhat greater in-flight-aspect ratio (IFAR) combined with qualitative and quantitative changes in the hydrodynamics of the implosion history. We next discuss each of these main extrapolation areas, in turn.

If extrapolation into regimes of different pellet core entropies (hence, different temperatures and temperature gradients), area (1) or (2), were to affect capsule performance in the HSC regime, the physics involved would probably be preheating, energy transport, and/or charged-particle coupling. For the purposes of this work, we assume that preheat control is primarily a matter of controlling the hohlraum drive physics, and we defer discussion of obtaining the correct pulse shape and drive spectrum to the hohlraum physics section, below. Charged-particle coupling, however, we consider to be an intrinsic part of the capsule physics.

b(3) [redacted] The effect of this correction on capsule performance is to change charged-particle coupling and transport coefficients in a direction that makes ignition more difficult, resulting in a higher minimum energy requirement to achieve ignition or in a lower yield at a given driving energy, near ignition. This effect will be quantitatively discussed below in presenting the developmental model calculations (PCM).

SECRET/RD UNCLASSIFIED

UNCLASSIFIED SECRET/RD

Data from Nova[9] suggest that extrapolation to a higher convergence ratio, area (4), might lead to significant degradations in capsule performance. It is difficult to apply the Nova data to HSC implosions, however, because the implosion histories are qualitatively very different.

Physics issues arising in connection with extrapolation in IFAR and implosion history, area (5), are at least as difficult. The issues here are primarily those of fluid instabilities and mix. A recent overview of the status of this field is given by Mikaelian.[13] Although the field has advanced considerably in recent years, direct experimental data are still scarce, and theoretical modeling approaches are disparate, relatively untested, and controversial

Fig. 6. Gain curve for hydrodynamically-scaled capsules.

UNCLASSIFIED SECRET/RD

UNCLASSIFIED SECRET/RD

[redacted] The gains chosen to represent YOC = 1 were based on optimized, clean-1D LASNEX calculations and estimates for HSCs under near-optimum conditions, as discussed in the next section. The conditions of these calculations were compared with those calculated for the tested capsules to estimate the uncertainty in each extrapolation, as follows.

First, consider extrapolating the Nova capsule data point to HSC conditions. We estimate from relevant LASNEX calculations that it should be possible to shift this design toward HSC conditions by using cryogenic DT, more sophisticated pulse shaping, and a convergence ratio of about 30, to an HSC-like capsule having a 1D-calculated yield (gain) that is higher by a factor of 10 to 50. For the gain curve extrapolation, we assumed the capsule gain could increase by a factor of 10, which can be thought of as resulting from conservative design yielding YOC = 1 or from a more ambitious design yielding a YOC = 0.2. Since the implosion history of such a capsule is quite different from those of the Nova-tested gas capsule (100× lower fuel entropy, 3–4× higher convergence, 2–4× higher IFAR), we have increased the uncertainty of the extrapolated point by adding a factor of 3 in quadrature with the Nova data uncertainty. We cannot rule out, but weigh lightly, the possibility of performing an even more highly-optimized fully-HSC implosion using Nova, conceivably shifting the low-energy portion of the gain curve upward. At present, no self-consistent designs exist for such a target concept.

[redacted]

C. Optimized LASNEX calculations of HSC performance

The optimized, clean-1D LASNEX design calculations shown in Fig. 4 contain several physical models that have become "standard" for ICF target design calculations.[4,14,15] The basic models for hydrodynamics, equation of state, multigroup radiation diffusion, and thermal conduction are largely based on fairly well-known physics and have changed only in fairly subtle details in recent years. Enhancements have been developed in some areas, particularly radiation transport, but these have not caused fundamental changes in capsule designs or performance predictions. Some of these standard physics models have known limitations under some circumstances, the most obvious for capsules being the limitations of 1D (one-dimensional, spherical symmetry) calculations, i.e., the neglect of asymmetries and hydrodynamic instabilities. These show up in capsule performance as a performance degradation with respect to clean-1D, with a magnitude that varies according to the implosion conditions.

Certain parameter constraints have been applied to all the design calculations used in this work to try to remain within reasonable expectations for the effects of asymmetry and hydro instabilities. They are restrictions placed on (1) the maximum allowed radial convergence ratio (CR) of the hot spot (the initial capsule outer radius divided by the radius of the hot spot at ignition), and (2) the maximum allowed IFAR (the instantaneous shell radius divided by the shell thickness to the 1/e density points). We limited the hot-spot CR to a maximum of about 40 and the IFAR to a maximum of about 50. If higher values were allowed, the 1D-calculated yields

UNCLASSIFIED SECRET/RD

UNCLASSIFIED SECRET/RD

could be higher at lower drive energy. We know of no experimental evidence that indicates that higher values can be achieved, but this is one area where possible "upside potential" exists, if we have been too conservative in choosing these limits.

All capsule data that we know of falls at or below the clean-1D calculated yield. Therefore, we have taken the clean-1D design calculations as a reasonable goal for HSC capsules and have used them to establish a contour with an estimated 5–15% probability of exceeding the predicted gain.

D. Calculations using developmental models

Two developmental models have been used to perform sensitivity studies for the HSCs at various drive energies.

b(3)

Starting from the clean-1D capsule designs, we reoptimized the capsule drive pulse to obtain maximum gain using each of the two data-normalized models.

b(3)

E. The resulting capsule gain curve

The capsule gain curve that results from consideration of the available capsule data and calculations is overlaid on the data base in Fig. 6. In judging the location of the capsule gain curve, we have tried to avoid undue optimism or pessimism, but simply to accept the evidence of the current data base. We assumed, in terms of historical experience with LASNEX capsule performance predictions, that the highly optimized LASNEX design calculations provide reasonable goals for ICF, but that experimental performance is fairly unlikely to exceed the calculated gains. We considered the historical experience with predicted and postshot YOCs and the capsule driving energy uncertainties of the data base in locating the "most probable" contour of the capsule gain curve. The most probable location of the ignition cliff was strongly guided by the developmental modeling.

The uncertainties we chose were guided by the entire experimental and calculational data base. The region of the capsule gain curve least constrained by the data is that near the ignition cliff.

b(3)

However, we chose the uncertainty in required capsule absorbed energy in this region to be plus or minus a factor of 3, double the demonstrated modeling sensitivity. This assumption was deemed necessary, given the incompleteness of our understanding of implosion physics, the partial success of predicting known capsules (either with or without the developmental models), and the complete lack of data in or near this region.

III. HOHLRAUM EFFICIENCY

The hohlraum model contains four "efficiency factors" to describe the effects on hohlraum efficiency of (1) laser entrance hole closure, (2) x-ray conversion, (3) plasma filling and drive symmetry, and (4) laser-plasma instabilities (LPIs). The overall hohlraum efficiency is the product of these four efficiency factors. We note that factor (4) is, strictly speaking, not an efficiency, but rather a factor constructed to take into account the effect of the complex (LPI) processes involved on the drive energy required to accomplish a successful high gain design. Some of these processes are closely coupled, and other ways of factoring the efficiency could certainly be considered. For example, hole closure and filling often arise in similar parts of design space, since both involve plasma motions. These two processes were split in our model, since the LASNEX calculations performed to evaluate their effects are completely separate. We lumped filling and drive symmetry together, because they, too, are strongly coupled and our calculations to evaluate their effects on the hohlraum treat both effects simultaneously. The most important feature of the factorization chosen is that it must separate the physical processes so that the split of efficiencies is consistent. The products of the efficiencies must account once, and only once, for each of the loss mechanisms and predictive uncertainties. Naturally, our model clips each

UNCLASSIFIED SECRET/RD

UNCLASSIFIED SECRET/RD

of the efficiency factors at 100%, to prevent spurious generation of energy that would violate the First Law of Thermodynamics. We guarded against double-counting or miscounting of loss mechanisms and uncertainties by (1) constructing the model framework from the outset to facilitate complete-, single-counting, i.e., matching the factors and sub-model physics to the available calculations and data with a minimum of cross-connection, (2) testing the model's numerical performance with examples constructed to exhibit simple, quantifiable behavior, and (3) checking our "realistic" results against both integrated and differential experiments and calculations, wherever possible, as noted in the appropriate sections of the paper.

Incidentially, the results of a model like this, composed of "sub-model factors," should be independent of the exact factorization and the number of factors chosen. The more factors chosen, the smaller the contribution of each factor to the uncertainty of the final result. This can be seen rigorously by referring to a standard text on error propagation. Here, we briefly illustrate the general idea with a gedanken experiment using counting data. Suppose we collect 1000 counts in some nuclear counting experiment. Does the statistical uncertainty in the total number of counts depend upon whether the counting apparatus had one channel or 10 channels? Not if the apparatus is working and the analysis is done correctly. In the multichannel case, each channel is more uncertain than the total count. However, if one combines the results from individual channels using correct error analysis, the uncertainty in the total count is not affected by the partitioning of the data. Although the case we analyze in the present work is somewhat more difficult to divide and recombine than this simple counting example, we have made every effort to perform the subdivision and error propagation consistently, so the results are as fair and accurate as possible.

At the outset, it is worth noting that our calculations accounting for the various efficiency factors vary widely in completeness and rigor. Further, experimental data to establish hohlraum efficiencies have greater uncertainty than the capsule data base, since some of the quantities involved have never been directly measured! For example, the radiation energy absorbed by the capsule is inferred from hohlraum and capsule calculations, rather than being directly measured. This situation introduces systematic uncertainty into the scaling to HST conditions. A much worse case of incompleteness is seen below in the area of the effects of laser-plasma instabilities, where scaling data are crude and where self-consistent, complete theoretical models do not even exist.

Another fundamental characteristic of the target physics data base makes the hohlraum efficiency predictions for megajoule-class laser targets more uncertain than the capsule predictions: our only experience with laser-driven hohlraums is at the low-energy end of the gain curve.

b(3)

Thus, we are forced to extrapolate upward from the Nova regime, based entirely on available theory and computational capabilities, with all their unknowns and demonstrated partial inadequacies.

In this section, we assess the values and uncertainties of the hohlraum efficiency model parameters as well as we can through estimates and detailed calculations of some of the underlying target physics processes. The expected scaling and uncertainty of each efficiency factor is discussed next, followed by discussion of the resulting overall hohlraum coupling efficiency prediction.

A. X-ray conversion

Let us discuss x-ray conversion first, since it is an area with an extensive, published experimental and calculational data base and is a factor for which uncertainties can be derived relatively concretely. For the purposes of our model, we define the x-ray conversion efficiency as the energy emitted in x-rays normalized by the absorbed laser energy.

Prior to consulting the experiment-related data base, we considered the possible design space for HST hohlraums. The conditions to be expected in such hohlraums vary, depending upon specifics of the target design. For current megajoule-scale hohlraum designs, we expect overall pulse durations of 30–50 ns, with main-pulse durations of 3–10 ns and peak incident laser intensities of 1–10 $\times$ 10^{14} W/cm^2. The hohlraum efficiency will be most strongly determined by conditions during the main pulse, since that accounts for over half the incident energy.

A summary of the available x-ray conversion data has been published.[15] A missing part of the experimental data base is, of course, scaling to megajoule-sized plasmas and the long, shaped pulses required for high-performance HSTs. Here, we discuss three points that play a major role in setting our prediction of the scaling of x-ray conversion efficiency and its uncertainty to HST conditions.

UNCLASSIFIED SECRET/RD

UNCLASSIFIED SECRET/RD

One key experimental finding is the apparent dependence of conversion efficiency on illumination uniformity, reported by Goldstone et al.[16] This result has been carefully checked by multiple diagnostics and repeated experiments and finds some general reinforcement from experimental results reported elsewhere.[17] To this result we attribute the following significance: under some irradiation conditions that might be useful for a megajoule-scale hohlraum, x-ray conversions of up to 90% might be achievable. Of course, this experimental result is obtained under conditions far from the megajoule-HST regime and is not understood calculationally, so we cannot simply predict 90% conversion for a laboratory near-ignition or high-gain hohlraum target. Rather, we treat it as a reasonable possible outcome.

A second important feature of the existing data base is the reasonable modeling of Nova hohlraum data that has been achieved using x-ray conversion efficiencies measured on open targets. The standard "scale-1" Nova (and previous) hohlraum experiments are modeled at LLNL[8] using the x-ray conversion efficiency obtained in analogous open-target experiments (50%), and this produces a reasonable account of the hohlraum temperature scaling, using nominal LASNEX modeling for the rest of the hohlraum physics. This motivates the correspondence we assume between open-target x-ray conversion efficiency measurements and predicted hohlraum conversion efficiencies. Such a correspondence has also been motivated theoretically by Mead et al.[18]

The third point we take from the x-ray conversion data base is an estimated uncertainty level for x-ray conversion calculations. There are numerous modest discrepancies between experiments and calculations, both in details of the x-ray emission and in scaling of the conversion efficiency. Two specific instances of discrepancies in x-ray conversion scaling can be seen in the data base: a discrepancy of a factor of 1.5 to 2 at low intensity for small spot-size irradiations, and the failure to predict the factor of 1.5 improvement in x-ray conversion that is observed with uniform illumination. In the first case, the code predictions are optimistic, while in the second, the experimental emission is greater than that calculated using "standard" LASNEX modeling. Furthermore, many moderate (factor of 1.5 to 2) discrepancies are seen between detailed predictions of LASNEX modeling and experimental measurements,[15,16] contributing somewhat to the uncertainty in extrapolating calculations to the HST regime.

With this data base as background, we predict the x-ray conversion efficiencies plotted in Fig. 7 for HSTs.

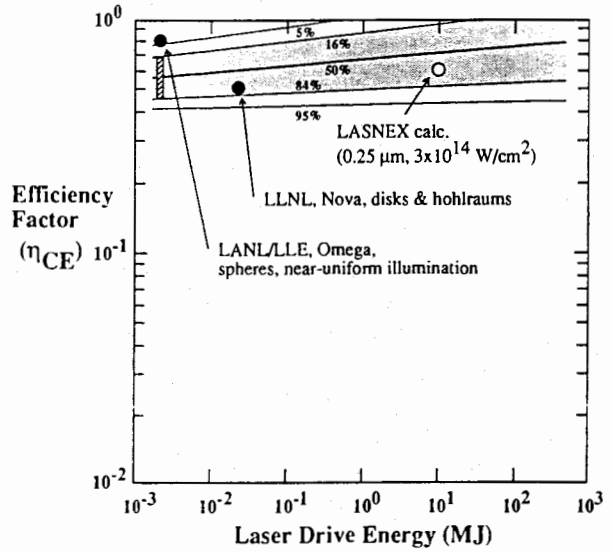

Fig. 7. X-ray conversion efficiency (η_{CE}) scaling.

At 10-MJ scale, we took the most probable value to be between the LASNEX-calculated prediction and the result that would be obtained if the highest experimental conversion efficiencies apply to these targets, and we included both outcomes within the 1σ uncertainty limits. We chose the gaussian form for the probability distribution functions based on the Central Limit Theorem and our assessment that these parameters are determined by a system having many degrees of freedom.

B. Laser entrance hole closure

The laser entrance hole (LEH) has to fulfill two conflicting requirements: (1) to admit the laser light to the desired part of the hohlraum and (2) to retain the x-ray drive in the hohlraum. If the hole is too small, there will be large light losses as the laser beam enters the hohlraum. If the hole is too large, there will be excessive radiation losses out the hole. Thus, some optimum in LEH size exists. We want to maximize the efficiency of the aperture, defined as the [(incident laser energy) − (prematurely absorbed energy) − (x-ray loss energy)] divided by the (incident laser energy). More rigorous calculations in the future should probably correct the x-ray loss term by the x-ray conversion efficiency. For the estimates of this section, we assume that laser-plasma instabilities in and near the entrance aperture are negligible.

UNCLASSIFIED SECRET/RD

UNCLASSIFIED SECRET/RD

Recent LASNEX calculations[19] suggest that laser entrance hole "closure" is a more subtle issue than our first estimates indicated. Early estimates[20] were based on motion of the critical surface contour and predicted that LEH closure was not a significant issue. Predictions of hohlraum performance at both LANL and LLNL have, in the past, neglected any efficiency loss associated with the laser entrance apertures for HSTs. However, our recent LASNEX calculations show that a potentially-important process has been neglected: the development (for megajoule-scale, pulse-shaped HSTs) of a large, tenuous plasma plume, originating from blowoff of the aperture lip and the adjacent hohlraum wall.* The extended plasma plume could absorb significant amounts of laser light before it enters the hohlraum. This premature absorption is a pulse-length- and scale-length-dependent phenomenon that is predicted by our calculations to be insignificant for current Nova hohlraums ($E_{Las} \simeq 20$ kJ, $\tau_{Las} \simeq 1$ ns, $R_{Hoh} \simeq 1$ mm) but potentially important for multimegajoule-scale HSTs (5–10 MJ, 30–80 ns, 1–2 cm).

b(3) [redacted] The calculational geometry is realistic, except that we use a numerical artifice (a plane of partial symmetry) to avoid high shear flows that cause the calculations to fail.

We have benchmarked the LASNEX hole-closure modeling against existing Nova LEH data. For a 1.0-scale Nova hohlraum,[8,9] irradiated by a 1-ns, flat-topped pulse, with an entrance aperture radius of 0.4 mm, we calculate a premature absorption of only about 5%. Estimates, both by hand and using LASNEX, suggest an x-ray loss of 10–12%. Thus our estimates based on hole-closure modeling for Nova suggest a loss of about 15% total, or an 85% aperture efficiency. This is consistent with available Nova data.[8,9] We note, however, that this test constrains the modeling only loosely.

The hole-closure calculations must be extrapolated from the current Nova target conditions to HST conditions, both at Nova size and at larger scales. Here, we discuss the extrapolations of the modeling to 10-MJ-HST target parameters and indicate how we estimated upper and lower 1σ limits for the prediction.

A reasonable estimate of a "pessimistic" limit for a 10-MJ HST is provided by the results of calculations using flux-limited diffusion. This model for radiation transport will overpredict the radiation flux on the lip of the entrance aperture, probably by a factor of about 2. In a simple approximation, this will cause about twice the appropriate mass flux to ablate and blow into the laser beam. We assume that this model, therefore, provides a reasonable safety factor for overall modeling uncertainties and use it to estimate a 1σ lower limit. We can obtain the lower 1σ limit we used from simulations of two different aperture sizes, as follows.

The LASNEX diffusion calculations for a 4-mm-radius LEH, using a pulse shape appropriate to a 10-MJ HST, give 54% absorption as the laser transits half of the plasma blowoff (thus approximating the "premature" absorption†). A simple estimate of the blackbody radiation loss from the aperture yields 1.4 MJ for two entrance ports. We derate this loss by a factor of 2, assuming that some significant closure of the aperture to x-ray losses occurs through a combination of hydrodynamic motion and the effects of strong laser deposition in the plasma near the aperture. This yields an estimate of 60% loss or 40% efficiency for a 4-mm entrance hole.

The LASNEX diffusion calculations for a 6-mm-radius entrance hole give about 35% absorption for the same laser pulse. In this case, we estimate about 25% radiation loss (derated here only a factor of 1.4 below the black-body limit, since the larger LEH will close fractionally less to the x-rays). Thus, we estimate for this case, too, about 60% losses, or about 40% efficiency.

b(3) [redacted] This model should more accurately calculate the x-ray flux on the lip of the aperture. The calculational geometry is likely to be optimistic, since it omits the constraints and plasma sources that would exist in an enclosed hohlraum target. The degree of optimism is dependent on how confined the hohlraum and hole-closure plasmas are and on the extent to which the plasma plume from the aperture itself would be enhanced by that confinement. We estimate, for a 10-MJ-HST aperture with 4-mm radius, that the laser absorption would be in the 5–15% range. This would imply an aperture efficiency perhaps as high as 85%, considering both the laser and x-ray losses. We take this as the plus-1σ limit.

Our conclusion, based upon our assessment of the current (limited) hole-closure data base, is that the laser entrance hole will most likely have an efficiency, for a 10-MJ HST, of about 40–85% as a result of premature laser light absorption and radiation losses out the hole after conversion to x-rays. We predict that the entrance hole efficiency decreases as the target scale (energy,

UNCLASSIFIED SECRET/RD

UNCLASSIFIED SECRET/RD

pulse length) increases, and we estimate that the prediction uncertainty increases as we extrapolate away from the current Nova experimental regime toward larger target scales. The resulting prediction and its uncertainties are shown in Fig. 8.

In this analysis, we have neglected two aspects of LEH design and physics. First, we have not included the (presently unknown) effect of designing the LEH with a low-Z liner to keep the aperture open. Calculations of this approach to date have yielded mixed results. In principle, a low-Z liner may improve the hole efficiency, but there is a delicate tradeoff between beneficial and deleterious effects to be made before the success of this approach can be assessed. Second, we have assumed that the effects of the laser entrance holes on the capsule drive symmetry can be controlled adequately. This may not be correct.

b(3)

We have design ideas that might permit approximate cancellation of the asymmetry. Pending further evaluation of this issue, we have ignored the effect for this gain curve analysis.

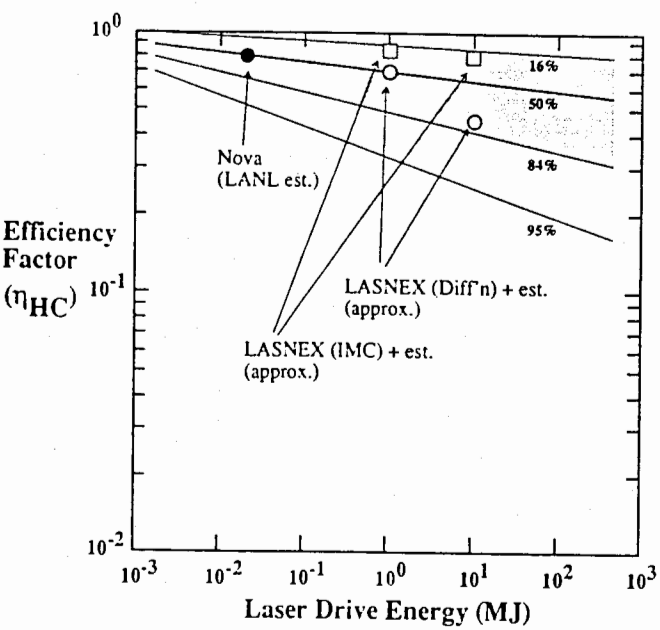

Fig. 8. Hole-closure efficiency factor (η_{HC}).

C. Plasma filling and drive asymmetry

The main function of the hohlraum in an x-ray-driven target is to provide a drive flux at the capsule that meets the spectral, temporal, and spatial requirements to obtain near-optimum capsule-implosion performance. In this section, we consider the energy penalty associated with producing adequate spatial uniformity of the drive flux. This is a complicated issue, since the capsule's tolerance to flux asymmetries varies throughout the drive pulse,[2] and the symmetry produced by the hohlraum is affected by motion of the hohlraum wall during the laser pulse (filling).

The task is further complicated because exact capsule symmetry requirements are not known.

b(3)

We shall ignore uncertainties in the capsule symmetry requirements in this analysis, an assumption that neglects some real uncertainty. Better treatment of this area may be possible in the future. It will be seen from the arguments below that considerable uncertainty arises in considering the hohlraum processes themselves, so perhaps the ignored uncertainty in the capsule tolerances is not important.

Here, as in the case of hole closure, the basic tradeoffs of hohlraum design are clear. The hohlraum must satisfy two intrinsically conflicting requirements: (1) to provide the needed drive pulse time-dependence, spectrum, and symmetry, consistent with good HSC implosion performance and (2) to do so with the maximum efficiency. For a given laser pulse shape, as the initial hohlraum size is made larger, the hohlraum becomes more effective at smoothing drive asymmetries. Conversely, as the hohlraum size chosen becomes smaller, the efficiency of delivering drive energy to the capsule becomes higher. Thus, in the simplest view, there is an optimum hohlraum size. We define the "symmetrization efficiency" of the hohlraum to be the radiation energy absorbed by the capsule (the x-ray drive energy) divided by the total x-ray energy available in the hohlraum. The hohlraum efficiency is dominantly determined by the wall loss incurred to produce adequate drive flux uniformity, which depends in turn upon the

UNCLASSIFIED

SECRET/RD

UNCLASSIFIED SECRET/RD

geometry and x-ray albedos of the case and capsule. Just as in the instance of entrance hole closure, this simple view can be further complicated in some cases by effects of laser-plasma interactions in the plasma within the hohlraum, discussed below. In this section, we ignore the possible effects of plasma instabilities.

Recent HST hohlraum design calculations[3] have indicated greater motion of the laser absorption and x-ray emission regions than had been anticipated from earlier design calculations. The cause is similar to the hole-closure effect: low-density, large-scalelength blowoff of high-Z material prematurely absorbs the laser light at a moving location, far from the initial hohlraum wall.[§] This motion of the absorption region leads to similar motion of the x-ray conversion or source region, leading to time-dependent drive asymmetries. Lindl[21] proposes that a low-Z liner may be needed to reduce such motion of the emission region, in order to reduce the time-shifting, drive-flux asymmetry at the capsule. Our hohlraum calculations[3] indicate that the concept has merit. However, at early times, the low-Z liner reduces the hohlraum wall albedo, making it more difficult to achieve good drive symmetry. Again, this design trade-off requires evaluation of delicate trade-offs of physical effects.

Our assessment of the hohlraum symmetry and filling data base follows a course somewhat parallel to that of hole closure. Here, too, we have Nova data at 1-ns pulse length, as interpreted by current LASNEX hohlraum modeling. We have LASNEX predictions of 1- to 10-MJ-scale HST hohlraum conditions. As in the case of hole closure, the LASNEX calculations contain known approximations and have clear inadequacies. For example, the hohlraum calculations have to be set up to prevent plasma motion near the laser entrance aperture in order to prevent numerical difficulties. This approximation at least has the benefit of helping to prevent double counting of premature absorption between hohlraum filling and hole-closure effects. Next, we discuss each of these data-base elements and our use of them in determining an HST hohlraum efficiency prediction.

The Nova hohlraum data base can be understood fairly quantitatively using LASNEX modeling. Suter et al. at LLNL have a multistep calculational model that appears to account adequately for most features of the Nova hohlraum drive conditions.[8] Magelssen et al. at Los Alamos have developed a particular one-step modeling technique using LASNEX that results in similar predictions for current Nova hohlraums.[3] Both models predict similar drive conditions, and both are generally consistent with available measurements within experimental uncertainties. The calculated hohlraum efficiency at Nova scale is about 22%, with significant (factor of plus-or-minus about 1.5) uncertainties because the inference is dependent upon unfolding via fairly crude calculations, and direct measurements are not available. The calculated time-averaged drive nonuniformity is about 5–10% peak-to-valley.

To scale the Nova data to HST conditions at 20-kJ laser energies, we make the following estimates. We estimate that a 20-kJ HSC would require an overall pulse length of 10–30 ns, with a main-pulse duration of 1–2 ns. We scale the required hohlraum size to account for (1) the longer laser pulse and (2) the need to achieve a factor of about 3 to 5 better drive symmetry. We estimate that the laser spot motion will increase by a factor of 3 to 5, increasing the effective source asymmetry by at least that same factor. With the source nonuniformity up by a factor of 3–5 and the required drive symmetry down by the same amount, it is necessary to achieve a factor of at least 10 improved smoothing. Using Haan's simple radiation smoothing model,[22] we estimate that this can be achieved for an $l = 4$ mode by increasing the case-to-capsule-radius ratio from about 3 to about 4.5. This, in turn, will decrease the hohlraum efficiency by a factor of about 2. Thus, we estimate a nominal hohlraum symmetrization efficiency of about 10% for 20-kJ HSC conditions. The uncertainties of this estimate are large (say, a factor of 1.5) and have been added in quadrature with the (factor of 1.5) uncertainty inferred for the current Nova conditions, yielding an overall uncertainty of plus-or-minus a factor of about 2.

To guide us at 1- and 10-MJ scales, we performed LASNEX point design calculations, including the effects of a (non-optimized) low-Z liner.[3] The calculations predict slightly higher symmetrization efficiencies at larger scales. This increase occurs as a result of gradually increasing pulse duration at higher drive energies ($\tau \sim E_L^{1/3}$) and the consequent increase in predicted wall albedos.

[redacted] b(3)

The calculations shown may not be optimum for hohlraum symmetry, so there is upside potential; but the design at present does not rigorously meet the drive symmetry requirements of the capsule, so there is downside risk.

UNCLASSIFIED SECRET/RD

UNCLASSIFIED SECRETARD

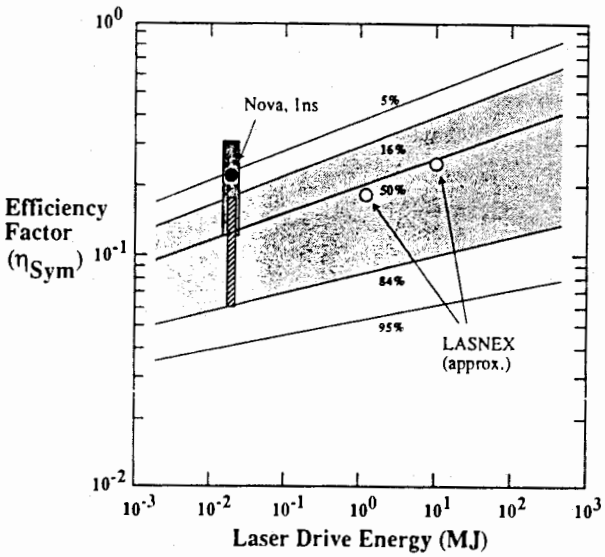

Fig. 9. Scaling of efficiency factor accounting for plasma filling and drive symmetry (η_{Sym}).

The results of these calculations and estimates are plotted in Fig. 9, together with the scaling chosen for the symmetrization efficiency and its estimated uncertainty. This area of hohlraum performance contributed the largest single (predicted) inefficiency and uncertainty to the prediction of future HSTs.

D. Laser-plasma instabilities

The behavior and effects of laser-plasma instabilities (LPIs) have long been of some concern to the design of high-gain ICF targets. The issue that has received the most attention is this: under some conditions, instabilities such as Stimulated Raman Scattering (SRS), can produce a population of hot (suprathermal) electrons that could cause serious preheating to the capsule interior, degrading the compression or requiring greater drive energy to achieve a specified capsule performance.[23] Other degradations might be produced as well. Here, we mention two examples. If Stimulated Brillouin Scattering (SBS) occurred in the plasma around the laser entrance aperture, this could decrease the useful absorbed energy in the hohlraum. Even in a less severe case of SBS, one might find changes in the illumination pattern on the hohlraum wall that would be difficult to predict and/or control. As another example, we speculate that self-focusing or filamentation of the laser light could change the x-ray conversion efficiency of a smooth beam by introducing large intensity modulations. To be quantitative about the possible effects of LPIs is difficult, because our theoretical understanding is inadequate in two areas: (1) predicting the plasma conditions in an HST hohlraum and (2) predicting the global behavior of the many instabilities under specified, complicated plasma conditions.

The behavior of LPIs is understood, ex post facto, in Nova target experiments using pulses about 1 ns in duration at laser energies up to 20 kJ. Current Nova hohlraum designs have fairly benign hot-electron signatures. SBS occurs at modest levels. Thin foil targets of low- and high-Z have illustrated the dependence of SBS on plasma scalelength and collisionality,[24] as expected from theory. The scaling of LPIs and hot-electron production with laser irradiation conditions is broadly understood within the Nova parameter space explored to date.

However, we expect three important factors to change the plasma conditions significantly in future HSTs, compared with those of present targets. First, HSTs require long, shaped pulses and therefore lead to the production of larger plasmas than seen in current targets. The pulse duration of an HST can easily be 30–50 ns, compared with current Nova pulse lengths of 1–3 ns. This could, depending on target design, extend plasma scalelengths by a factor of 5 to 30 from current experiments. Second, we are interested in predicting HST behavior at large laser energies. Assuming hydrodynamic scaling of plasma size with laser energy, the plasma size (and scalelength) could increase by a factor of order $(10\ \mathrm{MJ}/20\ \mathrm{kJ})^{1/3}$, or about 8. There is no way to simulate accurately a high-energy laser plasma with a small laser. The high-energy plasma will have larger spatial extent, higher temperatures, and longer dwell-times than can be obtained simultaneously using a smaller laser. Third, we expect that HSTs may require a low-Z liner to control asymmetry produced by motion of the laser spot and possibly to reduce laser entrance hole closure. Increasing the plasma scalelength, size, temperature, and dwell-time and decreasing the plasma Z are changes that increase the likelihood of strong effects due to LPIs.

To estimate the effects on HST performance of hot electrons produced by LPIs, we have made the following assumptions and calculations. We assume the plasma size and scalelength vary with laser energy and pulse duration according to hydrodynamic scaling, i.e., $L \sim \tau \sim E^{1/3}$. We consider plasma processes that are growing convectively, i.e., that grow exponentially as the (normalized) plasma scalelength increases.

UNCLASSIFIED SECRETARD

We use current LASNEX calculations to estimate actual plasma sizes at Nova and megajoule-laser scales. Our calculations suggest that a 10-MJ HST will contain about 1 cm of plasma and that the plasma scalelength may be 10 times the plasma size, but with possible short-scalelength substructure, depending upon target design details. If the plasma traversed by the laser is high-Z, i.e., the hohlraum is unlined and the capsule blowoff does not impinge on the laser propagation path, we calculate that the plasma temperature could be in the range of 5–10 keV. If the plasma is low-Z, either as a result of a low-Z liner or of capsule blowoff, we calculate temperatures a little lower, say 3–5 keV. In either case, large regions of density about 0.1 times the critical density are likely.

We estimate the hot-electron tolerance of the target using typical capsule and hohlraum design calculations and a simple hot-electron deposition model. We assume a typical hot-electron temperature, 40 keV. Our hot-electron transport and deposition model is similar to that used by Rosen et al.[25] We account for a Maxwellian hot-electron distribution, simple case and capsule materials and geometry, and hot-electron ranges and albedos, and compute the energy deposition in the pusher-fuel layers of the capsule. We estimate the tolerance to hot electrons to be the fraction of the laser energy that, when converted into a 40-keV electron distribution, would deposit an energy density in the pusher and fuel that equals the Fermi degenerate energy density. Our calculations agree with the examples reported by Rosen et al. To apply the model to our current "10-MJ" HST design, which actually requires about 20 MJ of laser energy and delivers about 2 MJ to the capsule, we use the following relevant information: case-to-capsule-radius ratio equal to 5, capsule initial radius of 4 mm, and ablator ρr of 0.032 g/cm^2. The 40-keV-hot-electron temperature is about the worst case for penetrating the ablator. We calculate a hot-electron tolerance of 3–5%, i.e., a maximum of 1 MJ into 40 keV hot electrons out of 20 MJ incident.

Finally, to estimate how strong the LPIs are likely to be, we make threshold estimates for the key processes under the calculated conditions in current and megajoule-scale target designs. A survey of LPI thresholds suggests that SRS is probably the worst-case source for hot electrons under HST conditions. We estimate from SRS backscatter thresholds that the current Nova hohlraum conditions would not be expected to produce significant hot-electron fractions, because of the short density scalelengths, a finding consistent with the Nova hot-electron data.[24] Next we discuss our estimates for two interesting laser examples at about 10 MJ scale.

First, we considered a target illuminated by light with the projected properties of a KrF laser: 0.25-μm wavelength, bandwidth of about 0.5%, adequately smooth beams to limit the seeding of self-focusing and filamentation, and continuous pulse shape, consistent with keeping the laser intensity at about 10^{16} W/cm^2 in the laser entrance aperture and below 4×10^{14} at the hohlraum wall. Taking the broad range of conditions likely to be encountered by the laser beam in a hohlraum, assuming an infinite, homogeneous medium and assuming that the laser encounters low-Z ($Z = 4$) plasma, either from the capsule blowoff or from a case liner, we obtain intensity thresholds for SRS backscatter in the range of 3 to 10×10^{14} W/cm^2. With specific consideration of the high-intensity regions near the laser entrance hole, taking into account the interactions of many incoherent, overlapping beams, incident from a wide range of angles, our estimates suggest that the effective SRS threshold should be about 10^{16} W/cm^2. The actual intensities, in the absence of self-focusing or filamentation, should be near or below threshold. Thus, it appears likely that hot-electron production due to SRS would be at modest levels (probably below 3–5%) under these target and irradiation conditions.

Second, we consider a similar target irradiated by a scaled-up Nd:glass laser. We assume the following laser properties (comparable with the current state of the art): 0.35-μm wavelength, bandwidth of about 0.1%, low beam quality (4:1 peak-to-valley intensity fluctuations on spatial scales of 10–100 μm), and delivery of picket-fence pulses with restricted dynamic range (say 40:1, peak:foot). Picket-fence pulses would produce intensities much higher at early times than continuous pulses. Self-focusing and filamentation could occur during one or more of the later pickets.[26] Average intensity during the main pulse would probably be about 2 times higher than for continuous pulses. Local peak intensities during the main pulse could also be a factor of 2 to 4 above the average, due to laser beam nonuniformities. Self-focusing and/or filamentation during the main pulse could raise peak intensities by an additional factor of 10 or more.[27] The narrower bandwidth and longer wavelength lead to SRS backscatter thresholds as low as $1\text{–}3 \times 10^{13}$ W/cm^2. Thus, under these conditions, our prediction is that SRS backscatter thresholds will be exceeded by large amounts, leading to hot-electron production at levels potentially exceeding 5%. Modifications of the laser capabilities may be possible, but short of such laser design improvements,

UNCLASSIFIED SECRET/RD

we estimate that a significant energy penalty, perhaps a laser energy requirement increased by a factor of 2 to 4, would be incurred in redesigning the target to operate under these irradiation conditions.

Thus, we find that the assumption of broad bandwidth, together with the control of peak intensities in the target (using smooth beams and continuous pulse shaping), produces conditions that are unlikely to generate significant hot-electron fluxes below megajoule target scales. However, at megajoule drive energies or above, SRS backscatter is above applicable thresholds in a low-Z-lined HST, unless optimum driver conditions are achieved, i.e., broad bandwidth (0.5%), short wavelength (0.25 μm), smooth beams (say 1.2:1 peak-to-valley), and continuous drive pulses. Under these conditions, there appears to be only moderate risk that hot electrons would preheat the capsule significantly. The maximum target degradation that would be expected under the most favorable irradiation conditions is such that an increase in laser energy (with target redesign, e.g., a larger hohlraum and/or a thicker capsule ablator) by a factor of 2 should compensate for the performance degradation. We have heuristically combined the various estimates and calculations for the KrF case into the probability band indicated in Fig. 10.

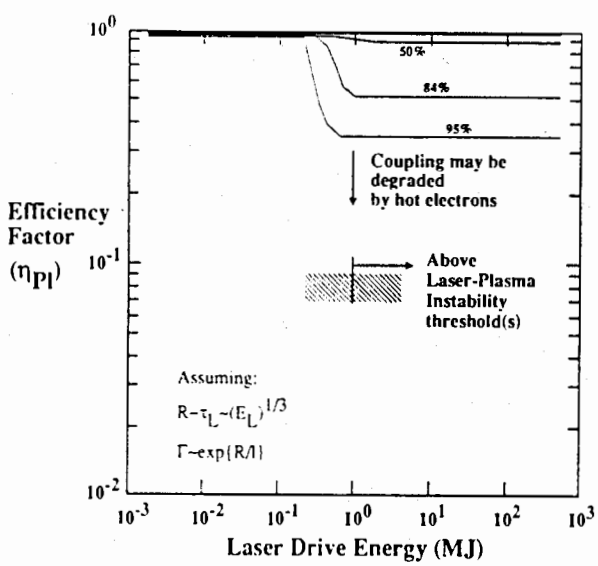

Fig. 10. Efficiency factor (η_{PI}) estimated to account for effects of laser-plasma instabilities, for the case with 0.5% band-width and smoothed 0.25-μm beams (KrF).

Perhaps more important than the specific prediction we have made here are these facts encountered in constructing the prediction:

- Closed-form prediction of LPI behavior in megajoule HSTs is not possible,
- If the laser beams interact with low-Z plasma, either at the entrance aperture or in the hohlraum volume, many LPIs will be far above threshold for a narrow-bandwidth laser at expected intensities, and
- Short wavelength, broad bandwidth, smooth beams, and continuous pulse shapes can reduce the risks and/or effects of LPIs on target performance significantly.

We believe these findings are unlikely to be fundamentally changed by experiments and theory based on existing facilities. The predictions need to be tested by constructing and applying a large laser facility to driving HSTs at megajoule- (near-ignition-) scale.

We note that, since the "efficiency" factor resulting from the effects of laser-plasma instabilities (LPIs) is not truly an efficiency, limiting this factor to 1.0 is not motivated by energy conservation. Instead, this limit arises from the fact that no one has demonstrated, by either estimates or detailed calculations, a significant performance improvement due to the effects of LPIs!

E. Overall hohlraum efficiency

Our hohlraum efficiency scaling model (see Appendix A) allows us to independently set each of the four efficiency parameters and their uncertainties to fit the values motivated above. The resulting product of the four factors is shown in Fig. 11. We can perform a final "test of reasonableness" by comparing the overall efficiency result to state-of-the-art LASNEX predictions for hohlraums, adjusted separately by estimates for the physics not taken into account by LASNEX. The open circles show the resulting cross-check at 1- and 10-MJ laser energies.

We can also apply our best scaling estimates to existing short-pulse Nova hohlraum data to estimate a hohlraum efficiency prediction for HSTs at 20-kJ laser energy. We extrapolated the Nova data assuming that the driving pulse would have to be increased by a factor of 3 to 30 from current 1–3 ns experiments and that the driving flux asymmetry would have to be reduced from the currently-inferred levels[8,9] of 5–10% by a factor of 2 to 3. With those assumptions, we estimate that

UNCLASSIFIED SECRET/RD

UNCLASSIFIED SECRET/RD

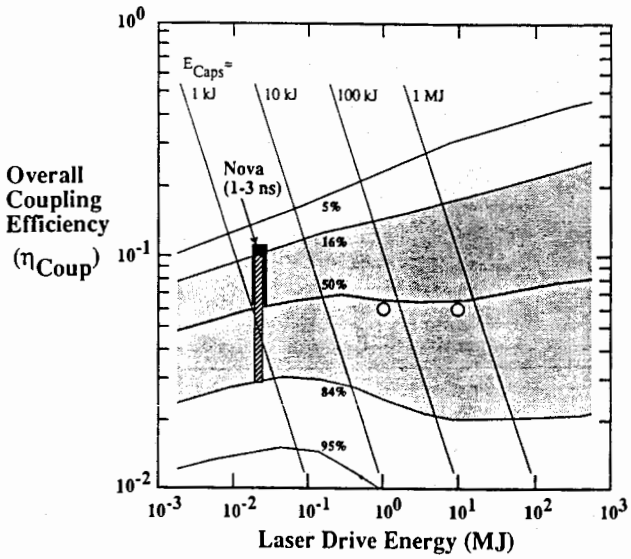

Fig. 11. Scaling of overall coupling efficiency (η_{Coup}).

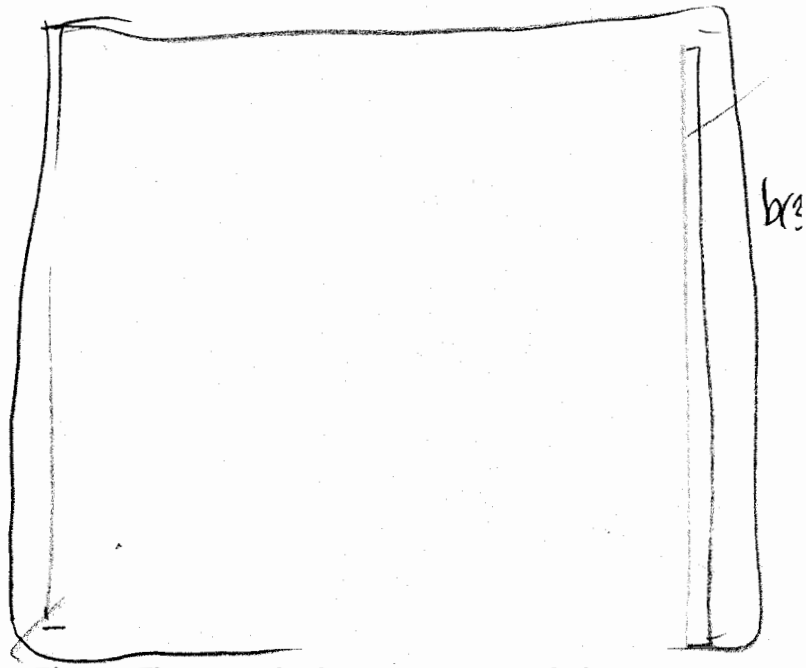

Fig. 12. The constrained Monte Carlo calculation combines parameter values and uncertainties to obtain gain curve probabilities.

hohlraum coupling efficiency for a 20-kJ HST would probably be in the range of 3–9%. We note, however, that realization of such a target on Nova would be a formidable technical challenge, even if feasible.

IV. OVERALL MODEL PREDICTIONS

A. Target gain prediction for the current data base

We have completed our discussion of the target physics data-base inputs to our target gain model. In this section, we show the results obtained using Monte Carlo calculations to enumerate and summarize the resulting family of possible outcomes. The procedure from here forward is a brute-force calculation of the propagation of uncertainties, together with a capability for asking what effects certain hypothetical data constraints would have on the resulting gain-curve predictions.

We assume, in performing the composite prediction, that the parameters and uncertainties embedded in each aspect of the model represent independent degrees of freedom; i.e., they represent possible outcomes for each of the processes modeled, without significant correlations among the process outcomes.# Note that if such correlations did exist, the result could be either a narrowing or a broadening of the error bars, depending on the details of the correlation. In the absence of strong correlations, we will obtain a reasonable estimate of the probability distribution of target gain predictions, within the context set by our input assumptions.

As an example of the resulting family of target gain curves, Fig. 12 shows 50 sample curves. We find no cases among those examined that lie outside the limits that could be expected, given our capsule gain and efficiency assumptions.

The final target gain prediction is shown in Fig. 13. Recall that the assumptions made in constructing this gain curve assumed KrF laser light, or equivalent. The contours show the probability that target gain will exceed the plotted value. For example, we predict a 50% probability of exceeding a target gain of about 8 for 10-MJ drive energy.

The gain distribution shown in Fig. 13 was obtained by computing a distribution function for 3200 independent Monte Carlo cases. The numerical uncertainty in the prediction is less than 2%, completely negligible compared with the uncertainties due to the physics inputs. As a final check, we have hand-estimated the cross-hatched band shown for a 20-kJ-scale HST. It agrees well with the results of the Monte Carlo calculation.

We have performed a number of numerical checks, some of which are presented in Table II. These tests show that 3200 Monte Carlo events are adequate to yield low

UNCLASSIFIED SECRET/RD

UNCLASSIFIED SECRET/RD

b(3)

Fig. 13. Predicted gain curve for hydrodynamically-scaled targets has large uncertainties that result from remaining target physics issues.

statistical errors. Also, they show that changing the cut-off of the gaussian probability distribution functions from 1σ to 3σ leads to only moderate changes in the predicted gain curve. The largest change here is a narrowing of the uncertainty contours and a slight shift in the median gain value (1.6 times higher at 10 MJ), if the parameter excursions are all limited to 1σ. We also find that the contours shift only moderately when the shape of the distribution function is changed by simultaneously increasing σ and decreasing the tail cut-off in compensating manner. These tests indicate that the median of the gain curve prediction is fairly independent of the exact shape and cut-off of the probability distribution functions. The tests also indicate, as they should, that changes in the width of the distribution functions, while maintaining fixed shape, do strongly alter the width of the composite prediction. We assume, without testing, that systematic, large skewing of the individual distribution functions would produce a change in the median gain. However, we currently see no mechanism that would produce significant skewing, beyond the small skews already discussed in connection with limiting the efficiency factors to 1, an effect we believe to be physical.

At first, one may be surprised by the size of the overall predicted uncertainty and the low target gain values that lie on the "most probable" (or 50%-probability) contour. Let us try to reach a global understanding of the meaning of this result.

First, let us observe that the uncertainty is large because it is the combination of many substantial uncertainties in the individual target physics processes. The magnitude of the uncertainty can be semiquantitatively obtained from hand estimates based on the physics inputs. Others may, of course, argue with the individual physics inputs or assumptions of the framework. Repositioning the curve's most probable (central) position would require only an appropriate change of one of the physics and design assumptions. However, to reduce the uncertainties, specific evidence must be developed to restrict the range of possible target physics scenarios.

Second, we note that the most probable gain curve is influenced primarily by two sets of assumptions: (1) that the optimized 1D-clean LASNEX capsule yields are the highest obtainable, and (2) the individual most probable hohlraum efficiency factors. Given these assumptions and the limitation of efficiency factors to a maximum of 100%, the target gain is reduced by one-half of the predicted uncertainty, compared with the optimistic LASNEX calculation. Thus, if the target physics data base is improved in a way that reduces uncertainties without lowering the predicted optimum performance, the most probable gain prediction will increase.

Third, we ask whether the model assumptions produce any obvious, unjustifiable bias. We answered this question to our own satisfaction in two ways. First, as noted above, we constructed the model to provide a framework that is as rigorous and consistent as possible. For areas where we necessarily invoked judgment, we listed and discussed with others the assumptions we considered potentially "optimistic" and those we considered potentially "pessimistic." From our viewpoint, these lists appeared to represent, qualitatively, about equal risks of over- or under-prediction. Second, we examined the results of the Monte Carlo calculations using estimates based on error propagation theory, and were able to verify code functionality. For the cases presented here in Figs. 7–11, the efficiency clipping at 100% does produce about a 30% downward shift of the median overall coupling efficiency. This shift is not produced by loss of high-efficiency events, since we retained all events, but rather by the slight magnitude imbalance between events above and below the median when the clipping occurs. That this result is at least approximately correct can be seen by testing the code where clipping does not occur, and by examining the extent to which the distribution

UNCLASSIFIED SECRET/RD

UNCLASSIFIED SECRET/RD

TABLE II. Summary of numerical test cases.[a]

Independent Variable Values				Gain at Probability =						
Run No.	ncas	SigCut	WMul	0.95	0.90	0.84	0.50	0.16	0.10	0.05
279	800	2	1	0.004	0.017	0.070	6.14	32.8	43.3	75.6
280	1600	2	1	0.006	0.023	0.093	6.14	32.8	43.3	75.6
281	3200	2	1	0.004	0.023	0.070	6.14	32.8	43.3	75.6
287	6400	2	1	0.004	0.023	0.093	6.14	32.8	43.3	75.6
283	3200	3	1	0.002	0.013	0.070	6.14	32.8	43.3	75.6
285	3200	1.5	1	0.02	0.093	0.38	8.11	32.8	43.3	57.2
286	3200	1	1	0.22	0.87	2.0	10.7	24.8	32.8	43.3
289	3200	1	2	0.001	0.006	0.023	4.64	32.8	57.2	75.6
291	3200	2	2	9×10^{-6}	3×10^{-4}	0.001	2.00	32.8	57.2	100
293	3200	2	2	3×10^{-4}	0.003	0.017	6.14	32.8	57.2	75.6

[a]The independent variables were ncas, the number of Monte Carlo vectors generated; SigCut, the cutoff in units of sigma for the event generator; and WMul, a multiplier on the nominal probability distribution function widths (applied to all submodel sigmas). Tabulated results are the gain values for 10-MJ laser drive energy at the probability contours of 0.95 to 0.05. We consider run 281 as the "reference case." Varying ncas (runs 279-281) checks the statistical error in the results. Varying SigMul (compare runs 281, 283, 285–286), we explored the effects of the probability function tails. Comparing runs with constant SigCut × WMul allows exploring the sensitivity of the calculation to the shape of the distribution function while holding the physical cutoff of the distribution functions fixed (compare runs 281, 289). Flattening the distribution function out to the 1-sigma limit broadens the gain curve uncertainty band. Using WMul alone (run 291—all model parameters; run 293—efficiency factors only) shows the dependence of the results on changes in all the individual processes' uncertainties (this dependence should be fairly strong).

function clipping could be expected to shift the median in the "realistic" case. On the basis of these tests and checks, we conclude that the results contain no obvious, unphysical bias.

To aid in interpreting this gain curve, an example may be useful. Suppose that one wishes to obtain a target yield of greater than 100 MJ, with a confidence level of about 85%. How large a laser should one construct, given the current uncertainty in the gain curve? Tracing the 100-MJ yield line to where it intercepts the 84% probability contour, we find that the laser should supply about 60 MJ to the target. With this as a guide, different tradeoffs among yield, tolerable risk level, and driver size can be considered.

B. Effects of successful future experiments on gain curve

Using the framework provided by this model, we can examine the effects of hypothetical future experiments on the target gain curve. One can intuitively expect that further knowledge (or constraints) added to the data base will both reduce the uncertainty band (unless the experiments are inconsistent with the existing data base!) and shift the most probable predicted gain. We shall discuss three specific examples (scenarios) here.

The first scenario, shown in Fig. 14, shows the effect on the gain curve of performing "successful" HST target experiments using hypothetical 100-kJ and 1-MJ laser facilities. The left-hand panel shows the gain curve

UNCLASSIFIED

SECRET/RD

UNCLASSIFIED SECRET/RD

Fig. 14. Experiments with HSTs will reduce gain-curve uncertainties and may redefine its shape and location.

predicted using the current data base. For the central panel, we assumed that an HST was successfully fielded on a 100-kJ facility and that the outcome of the experiment was at the 16% contour of the current data base. We assumed that the data uncertainty was plus or minus a factor of 2 in gain at 100-kJ laser energy. The result is to reduce the uncertainty band by a large amount below or near 100 kJ and by a lesser amount as one must extrapolate above 100 kJ. The right-hand panel shows the further "squeeze" that results if one then successfully completes an HST experiment at 1-MJ of laser energy.

The effects on the gain curve can be displayed more simply if we ask a question such as, "How large a laser needs to be built to obtain a yield of 100 MJ at 90% confidence level?" This question is typical of those being asked in current planning discussions of the Laboratory Microfusion Facility (LMF). The question has different answers, depending upon the status of the target physics data base as shown in Fig. 15. The point plotted as a "+" gives the answer derived above: about 60 MJ. The two open circles show the answers, given the target physics data base enhancements that would be produced by successful HST experiments at 100-kJ and 1-MJ facilities, as discussed in detail in the first scenario above. Successful HST experiments at 1-MJ energy would reduce the required LMF energy to about 10 MJ. This reduction of required LMF energy from 60 MJ to 10 MJ can be thought of as the "payoff" for building the 1-MJ facility and executing the successful experiments. Of course, if the experiments at 1 MJ were not successful, the required LMF laser energy could increase, depending upon the reasons for the failure. Here, the "payoff" of the 1-MJ experiments would be avoidance of an unsuccessful LMF, and program redirection. Other risk-benefit-outcome analyses are possible using this framework.

UNCLASSIFIED SECRET/RD

UNCLASSIFIED SECRET/RD

b(3)

We close this section with a third scenario that can be read directly from the results of Fig. 14: a high-risk LMF example. Suppose one declared the LMF to be a "research facility" and accepted only a 50% probability of achieving yield 100 MJ. With the current data base and the favorable beam properties expected for a KrF laser (left panel of Fig. 14), one could decide to build a 10-MJ facility. We note that this is likely to be a "high-end" research facility, so its cost-benefit levels would have to be carefully evaluated.

V. CONCLUSIONS

We have developed a new methodology for making quantitative predictions of future HST experiments. We used a model framework that separates target physics into independent processes, then parametrizes those processes using the best available data and calculations. The procedure allows a physics-data-based prediction of HST gain curves and their associated uncertainty.

This conceptual framework provides the most carefully constructed, conceptually consistent ICF gain curve to date. Nonetheless, the conceptual clarity of the framework has revealed areas where specific answers to important questions can at present be obtained only by using simple estimates and quite a bit of judgment. These missing pieces of information lead to arguable assumptions that can be tested only by future advances in theory, design, and experiment. For now, these areas of missing knowledge show up quantitatively as uncertainty in the gain curve prediction.

We evaluated the available target physics data base and set the model parameters accordingly. In the process, we highlighted areas of greatest uncertainty: capsule gain near the ignition cliff, hohlraum energy penalty incurred to obtain the required drive symmetry, and behavior of laser-plasma instabilities at megajoule target scale. Other processes such as x-ray conversion and hole closure contribute lesser, though significant, uncertainties. We found that the use of a low-Z liner is desirable for control of laser spot motion and drive asymmetries (filling), but that this increases the likelihood of serious LPIs. Estimates indicate that the risks of degradation due to LPIs are significant, unless one uses a laser driver that can produce 0.25-μm light with broad-bandwidth (0.5%), smooth beams, and continuous, wide-dynamic-range pulse shapes.

We found that the current capsule physics data base leads to about a factor of plus or minus 3 uncertainty in the energy location of the ignition cliff. We found that hohlraum processes exhibit somewhat greater overall uncertainty, increasing the uncertainty at the target ignition cliff to about plus or minus a factor of 5 to 6 in laser energy.

The large uncertainties of the current data base imply that achieving the LMF-defined goal of 100-MJ yield with 90% confidence level using a KrF laser facility would currently require construction of a 60-MJ facility. This energy requirement could easily be a factor of 2–4 (or more) higher using the current laser capabilities of Nd:glass. We found that extending the target physics data base with successful HST experiments could substantially reduce the required laser size to achieve a given gain/confidence performance level. For example, success with a 1-MJ HST experiment could reduce the required facility energy to 10 MJ for this case.

b(3)

Such experiments would, therefore, help to determine ICF feasibility at lower cost than a leap to the LMF under the current high-risk or high-energy scenarios.

Having completed the present work, one immediately recognizes a number of refinements that could improve its rigor. Some examples have already arisen: quantitative treatment of extrapolation uncertainties, possibly by defining a weighted extrapolation metric; better form and tighter rationale for the laser-plasma-instability scaling function; and perhaps a more extensive breakdown of the target physics processes, combined with extensive sensitivity studies to estimate uncertainties as function of drive energy. We suspect that repairing these inadequacies is unlikely to change the overall conclusions of this work. The highest leverage we see to reduce uncertainties is moving experiments toward the desired parameter regime for HSTs, testing theories and

SECRET/RD UNCLASSIFIED

UNCLASSIFIED SECRET/RD

calculation further, and adding firm constraints at higher laser/target energies.

APPENDIX A: DETAILS OF THE MODEL

The overall gain curve model has been described in the main text, and a schematic of the model and its basic notation are shown in Fig. 1. This appendix presents details of the capsule gain model and the hohlraum efficiency model and some specific notes on the fitting procedure used in constructing the gain curve prediction.

A. Capsule gain model

The capsule gain model is a function of six adjustable parameters that simulates the scaling behavior of ICF capsules. The model, shown schematically in Fig. A1, has been constructed to fit the results of detailed LASNEX design calculations for HSCs. The capsule gain space is divided into three regions: pre-ignition (PI), bootstrapping (B), and high gain (HG). The bootstrapping region is further subdivided into halves for numerical convenience. The capsule gain function is constructed piecewise, as discussed below.

The pre-ignition regime is defined to extend from the smallest HSCs up to the "ignition capsule gain" G_{Ign}, at which bootstrapping (alpha self-heating of the fuel) begins. In the pre-ignition regime, the capsule gain is given by

$$G_{PI}\,(E_{Caps}) = G_0 \exp\,[\alpha_{PI}\,\ln\,(E_{Caps}/E_{C0})] \quad , \quad \text{(A1)}$$

where E_{Caps} is the radiation energy absorbed by the capsule, α_{PI} is the logarithmic slope of the gain curve in the pre-ignition regime, and G_0 is the capsule gain at absorbed energy E_{C0}.

The bootstrapping region begins when the capsule gain predicted by Eq. (A1) reaches G_{Ign}. This defines an ignition capsule drive energy, E_{Ign}, obtained by solving Eq. (A1) with $G_{PI}\,(E_{Ign}) = G_{Ign}$. The bootstrapping region itself has two equal-width subregions in capsule absorbed energy space. The lower bootstrapping region extends from E_{Ign} to a central energy,

$$E_{BC} = E_{Ign}\,10^{2W_B} \quad \text{(A2a)}$$

while the upper bootstrapping region extends from E_{BC} to

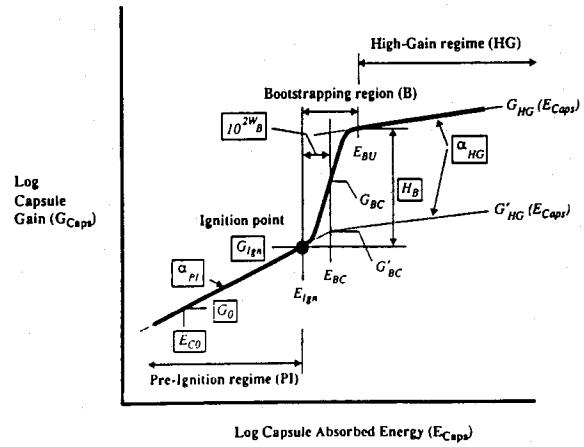

Fig. A1. Capsule gain model schematic. The seven input parameters are boxed for emphasis. The other parameters are derived quantities.

$$E_{BU} = E_{Ign}\,10^{4W_B} \quad \text{(A2b)}$$

where W_B is the e-folding half-width (in decades) of the bootstrapping region.

In the lower bootstrapping region, the capsule gain is given by

$$G_{BL}\,(E_{Caps}) = G_{PI}\,(E_{Caps})\,H_B^{0.5[1+\tanh(x_C)]} \quad \text{(A3)}$$

where H_B is the logarithmic full-height of the bootstrapping or ignition cliff and

$$x_C = [\log\,(E_{Caps}/E_{BC})]/W_B. \quad \text{(A4)}$$

The gain at the center of the bootstrapping region is then

$$G_{BC} = G_{PI}\,(E_{BC})H_B^{0.5}. \quad \text{(A5)}$$

To obtain an "invisible" transition from the pre-ignition to the high-gain slope, we place the slope change at the center of the bootstrapping region. We define a partial gain at the transition point, E_{BC}, as

$$G'_{BC} = G_0 \exp\,[\alpha_{PI}\,\ln\,(E_{BC}/E_{C0})]. \quad \text{(A6a)}$$

Then, whenever $E_{Caps} > E_{BC}$, we use the partial gain

$$G'_{HG}\,(E_{Caps}) = G'_{BC} \exp\,[\alpha_{HG}\,\ln(E_{Caps}/E_{BC})] \quad \text{(A6b)}$$

UNCLASSIFIED SECRET/RD

UNCLASSIFIED SECRET/RD

where α_{HG} is the logarithmic slope in the high-gain region.

The capsule gain in the upper bootstrapping region is

$$G_{BU}\left(E_{Caps}\right) = G'_{HG}\, H_B^{0.5[1+\tanh(x_C)]}. \qquad \text{(A7)}$$

Finally, in the high gain-region, the capsule gain is

$$G_{HG}\left(E_{Caps}\right) = G'_{HG}\left(E_{Caps}\right) H_B. \qquad \text{(A8)}$$

In summary, the capsule gain function can be written

$$G\left(E_{Caps}\right) = \begin{cases} G_0 \exp\left[\alpha_{PI} \ln\left(E_{Caps}/E_{C0}\right)\right] H_B^{0.5[1+\tanh(x_C)]} \;, & \text{for } E_{Caps} \le E_{BC} \;, \\ G'_{BC} \exp\left[\alpha_{HG} \ln\left(E_{Caps}/E_{BC}\right)\right] H_B^{0.5[1+\tanh(x_C)]} \;, & \text{for } E_{Caps} \ge E_{BC} \;, \end{cases} \qquad \text{(A9)}$$

where x_C is given by Eq. (A4). The six adjustable capsule-model parameters are G_0, α_{PI}, G_{Ign}, W_B, H_B, and α_{HG}. Although the model has a seventh parameter E_{C0}, in actual usage we treated E_{C0} as a fixed quantity. We assigned no uncertainty to it and did not adjust it to perform the fit to the capsule data base. Thus, we refer to the model as a six-parameter model.

The remainder of the capsule gain model consists of a Monte Carlo framework. Each parameter in the model has a corresponding (multiplicative) uncertainty, defined to be the 1σ width of a gaussian distribution function. We chose the gaussian form for the probability distribution functions based on the Central Limit Theorem and our assessment that these parameters are determined by a system having many degrees of freedom. The Monte Carlo mechanism is very simple, except for one subtlety that we incorporated after studying LASNEX-calculated capsule gain curves.

In analyzing LASNEX calculations of capsule gain curves computed with different physical models, we discovered that the features of the gain curve can display a definite correlation. Physical models that lead to higher gains at low capsule energies (higher G_0) generally lead to

- steeper gain slope in the pre-ignition region (increased α_{PI}),
- shift of the ignition point to higher gain, but lower energy (increased G_{Ign}),
- steeper bootstrapping cliff (decreased W_B),
- lower bootstrapping cliff-height (decreased H_B), and
- shallower slope in the high gain region (decreased α_{HG}).

We do not understand the cause of this correlation. It might arise as a result of fuel depletion or a shift in overall implosion timing.

We incorporated a correlation mechanism into the Monte Carlo generator that allowed us to choose the six random capsule-model variables with some correlation coefficient. We varied the correlation coefficient to test its effect, and found that it had some impact on the shape of individual gain curves, but very little impact on the shape of the mean or the uncertainty envelope of the predicted capsule gain curve. We finally adopted a correlation coefficient of 0.5, splitting the difference between complete correlation and no correlation.

B. Hohlraum efficiency model

The hohlraum efficiency model is a factorization of hohlraum processes that allows independent input of the values and scalings of individual process efficiencies. Each process is considered as an energy conversion step. We chose a particular factorization that separates five classes of hohlraum processes: (1) useful laser light absorption (i.e., light absorbed inside the hohlraum where it is useful for driving the capsule); (2) x-ray conversion; (3) x-ray losses from hohlraum apertures; (4) symmetrization and x-ray transport to the capsule; and (5) laser-plasma instabilities. In practice, (1) and (3) are very closely related, so we grouped the useful absorption and x-ray losses into a single process we call "laser entrance hole (LEH) closure." Note that laser plasma instabilities affect target performance before they actually affect energy transfer efficiency. In this case, we assign an "efficiency" that represents the energy-cost of design

UNCLASSIFIED SECRET/RD

UNCLASSIFIED SECRET/RD

modifications that would "fix" target degradations due to plasma instabilities. The hohlraum efficiency model contains a total of nine adjustable parameters (plus their uncertainties).

The overall hohlraum efficiency is then a product of efficiency factors for each of these process groupings,

$$\eta_{Coup}(E_T) = \eta_{CE}(E_T)\,\eta_{HC}(E_T)\,\eta_{Sym}(E_T)\,\eta_{Pl}(E_T) \quad . \tag{A10}$$

All of the process efficiencies except η_{PI} were scaled with the form

$$\eta_i(E_T) = \eta_{i0}\exp\left[\alpha_i \ln\left(E_T/E_0\right)\right] \quad , \tag{A11}$$

where i ranges over the processes (CE, HC, SYM), η_{i0} is the efficiency at E_0, and α_i is the logarithmic slope in laser (target-incident) energy space, E_T. Each efficiency is clipped to a maximum value of 1 to prevent spurious generation of energy that would violate the First Law of Thermodynamics. We note that, since the "efficiency" factor resulting from the effects of laser-plasma instabilities (LPIs) is not truly an efficiency, limiting this factor to 1.0 is not motivated by energy conservation. Instead, this limit arises from the fact that no one has demonstrated, by either estimates or detailed calculations, a significant performance improvement due to the effects of LPIs! This accounts for six of the nine adjustable, hohlraum-model parameters. Each of these six parameters has an associated (additive) uncertainty. The parameter E_0 is treated as a fixed, non-adjustable parameter and has no associated degree of freedom or uncertainty.

The "efficiency" assigned to plasma instabilities was scaled differently. The physical motivation for this choice of scaling is given in the main text. Operationally, we established a threshold function exactly analogous to that used for the capsule gain in the bootstrapping region,

$$\eta_{PI}(E_T) = H_{PI}^{0.5[1+\tanh(x_T)]} \quad , \tag{A12}$$

where

$$x_T = \left[\log\left(E_T/E_{PI0}\right)\right]/W_{PI} \quad . \tag{A13}$$

Thus, we describe the plasma efficiency as a cliff, controlled by its height H_{PI} (always less than 1 in this case), energy width W_{PI}, and position in energy space E_{PI0}. At low energies, this gives a plasma process "efficiency" of 1, as is desired to satisfy the physics rationale. At high energies, this relation gives a constant energy penalty. This may not be physically correct, since scaling the target up in energy above the threshold leads to complicated scaling of both the plasma processes and the tolerance of the target to the effects of the plasma processes. We lack more detailed knowledge of this scaling, so we use this simple form, which should be adequate near the threshold, in any case. This accounts for the final three adjustable parameters of the hohlraum efficiency model. For convenience, we define the uncertainties of these three parameters as multiplicative factors.

The Monte Carlo framework for the hohlraum efficiency model is very similar to that for the capsule gain model. Each of the nine parameters has an associated 1σ uncertainty, as described above. Here, we assume that all the model parameters are independent. In generating candidate gain curves, each of the nine parameters is assigned a random value with the appropriate probability distribution. The overall coupling efficiency is then calculated from the individual process efficiencies using Eq. (A9).

C. Fitting procedure

The inputs to the gain curve model were set by hand to match the constraints available from the target physics data base. We present a few details of the fitting procedure here.

The capsule gain curve fit was performed as follows. [redacted] b(3) This became a rough target for the $+1\sigma$ contour of the predicted gain curve. In the region of the cliff, we used the developmental modeling to estimate the energy uncertainty in that part of the curve, with a conservative factor of 2 to allow for inadequacies of the models. [redacted] b(3) From this data, we made estimates of the capsule gain model parameters. We then ran a series of Monte Carlo calculations, typically with 800–1600 gain curve samples each. We iteratively tuned the six adjustable capsule model parameters until a good fit was achieved to the available constraints. The fit appears to be fairly unique, given the form of the model and the constraints we used.

The hohlraum efficiency model parameters were similarly fit to their respective data constraints. In general, Nova hohlraum data established the efficiency values and uncertainties at the low end of the gain curve. The

UNCLASSIFIED SECRET/RD

UNCLASSIFIED SECRET/RD

scaling slopes were then set to match the predicted performance for 10-MJ HST calculations and estimates. In general, we estimated that the uncertainties increased gradually between Nova and the LMF, and we used whatever specific criteria we could generate to constrain the uncertainties at 10 MJ. Uncertainties in the efficiency slope parameters were chosen to fit the available constraints.

The plasma instability efficiency parameters were adjusted to fit the behavior motivated in the main text. As indicated in the text, the physical knowledge of plasma conditions and laser-plasma coupling instability behavior is not quantitative enough to make the fitting procedure critical.

The values used as input for each of the model parameters and the uncertainties are presented in Tables AI and AII for the capsule gain and hohlraum efficiency models, respectively. These values correspond with the "nominal" (KrF) predictions shown in Figs. 6, 7–11, and 13.

TABLE AII. Hohlraum efficiency model parameters and uncertainties for nominal "KrF" hohlraum prediction (see Figs. 7–11). For the η's and α's, the uncertainty is stated as an additive term at the 1σ level. For the plasma parameters, E_{Pl}, W_{Pl}, and H_{Pl}, the uncertainty is stated as a as a 1σ multiplicative factor.

Parameter	Parameter Value	Uncertainty
E_0	1×10^{-3}	–
η_{CE}	0.56	0.14
α_{CE}	0.025	0.022
η_{HC}	0.86	0.15
α_{HC}	0.035	0.033
η_{Sym}	0.10	0.05
α_{Sym}	0.105	0.0625
E_{Pl0}	1.0	5.0
W_{Pl}	0.33	3.0
H_{Pl}	0.9	3.0

ACKNOWLEDGMENTS

Useful discussions with D. DuBois, R. Kirkpatrick, W. Varnum, and D. Wilson of Los Alamos are appreciated. We also thank S. Haan, L. Suter, and J. Lindl of LLNL for useful comments and discussions throughout the course of this work, and we appreciate the stimulating discussions with W. Lokke, G. McCall, and, especially, D. Cartwright, who, in part, helped to launch this investigation. We thank D. Wilson and D. Cartwright for encouragement and support.

Work performed under the auspices of the US Department of Energy by the Los Alamos National Laboratory under contract number W-7405-ENG-36.

TABLE AI. Capsule gain model parameters and uncertainties for nominal capsule gain curve (see Fig. 6). For each parameter, the uncertainty is stated as a multiplicative factor at the 1σ level.

Parameter	Parameter Value	Uncertainty
E_{C0}	1×10^{-3}	–
G_0	1×10^{-4}	6.0
α_{PI}	1.9	1.125
G_{Ign}	0.4	4.0
W_B	0.25	3.0
B	25	4.0
α_{HG}	0.2	1.5

---

* For consistency, we have defined the entrance aperture to include some of the hohlraum wall surrounding the hole, a portion of the wall that is not properly treated in the hohlraum filling calculations because of numerical difficulties.

† At the entrance to an actual hohlraum, there would be premature absorption in the plume extending outside beyond the LEH, and also in the plasma immediately inside the LEH. The absorption calculated by LASNEX in the semi-symmetric problem (symmetric hydro and radiation physics, with 1/2-transit by the laser light) is the best approximation available at present to the sum of these two processes. This approximation should be good to within a factor of 2.

§ W. L. Kruer made early estimates (private communication, 1982) indicating the potential for absorption of the laser light in low-density plasma in large

UNCLASSIFIED SECRET/RD

UNCLASSIFIED SECRET/RD

targets, but the impact of the effect on symmetry was not immediately appreciated.

The exception to the "no-correlation" assumption is the partial correlation among parameters devised for the capsule gain model, discussed in more detail in Appendix A.

1. J. D. Lindl and W. C. Mead, Phys. Rev. Lett. **34**, 1273 (1975).
2. S. V. Coggeshall and W. C. Mead, "Single Shell DT/Foam Reactor Target: Physics and Issues (SRD)," Los Alamos National Laboratory report X-1-87-46 (SRD) (1987), and Def. Res. Rev. **1**, No. 4, 41 (SRD) (1989); S. V. Coggeshall and W. C. Mead, "Single Shell Foam Capsule Design (U)," Los Alamos National Laboratory report X-1-90-076 (SRD) (1990) and to be published in *Proceedings of JOWOG 37* (U), Sandia National Laboratories, January 22–25 (SRD) (1990).
3. G. R. Magelssen, M. Cray, S. V. Coggeshall, R. D. Jones, W. C. Mead, C. A. Wingate, and D. C. Wilson, "Radiation Symmetry within Laser Hohlraums (U)," Los Alamos National Laboratory report LA-CP-X-1-90-039 (SRD) (1990) and to be published in *Proceedings of JOWOG 37* (U), Sandia National Laboratories, January 22-25 (SRD) (1990).
4. G. B. Zimmerman, Lawrence Livermore Laboratory report UCRL-75881 (1974); G. B. Zimmerman and W. L Kruer, Comm. Plasma Phys. and Contr. Fusion **2**, 51 (1975); R. M. More and G. B. Zimmerman, Lawrence Livermore Laboratory report UCRL 50021-79, (1980) pp. 3-66–3-72.
5. J. H. Nuckolls and J. D. Lindl, private communication (1977–1983); J. H. Nuckolls, "Reactor Gain Curves (U)," in *Laser Program Annual Report–1978*, edited by M. J. Monsler, Lawrence Livermore Laboratory report UCRL 50055-78 (SRD) (1979), pp. 2-4 to 2-5; J. D. Lindl, L. W. Coleman, and E. K. Storm, "Recent Progress toward High-Gain Laboratory ICF (U)," in *Laser Program Annual Report–1986/87*, Lawrence Livermore National Laboratory report UCRL 50055-86/87 (SRD) (1988), pp. 1-3 to 1-29; E. K. Storm, "Summary and Conclusion (U)," in *Target Physics Review*, Lawrence Livermore National Laboratory report CLYC 88-0023A, (SRD) (1988), pp. 289 ff.
6. R. A. Sacks and J. D. Lindl, "Gain Systematics for Indirectly Driven ICF Laser Targets (U)," Lawrence Livermore National Laboratory report XDIV 90-0026 (SRD) (1990); also Def. Res. Rev. **2**, No. 3 (SRD) (October 1990), p. 100.
7. [redacted] b(3)
8. L. J. Suter, private communication (1987–89).
9. J. D. Kilkenny, "Nova Capsule Experiments (U)," in *Target Physics Review* (U), Lawrence Livermore National Laboratory report CLYC 88-0023A (SRD) (1988), pp. 185ff; S. P. Hatchett, "The Nova Implosion Program ... (U)," loc. cit., pp. 219 ff.
10. [redacted] b(3
11. H. N. Fisher, "Effects of Plasma Coupling on Burn Physics (U)," Los Alamos National Laboratory report LA-CR-89-79 (1989), and in *Proceedings of the 1989 Topical Conference on the Physics of Radiatively Driven ICF Targets* (U), edited by E. M. Campbell and R. L. Kauffman, Lawrence Livermore National Laboratory report CLYE 89-0004 (SRD) (1989).
12. [redacted] b(
13. K. O. Mikaelian, Def. Res. Rev. **1**, No. 2 (SRD) (1989), p. 91.
14. W. C. Mead, E. M. Campbell, W. L. Kruer et al., Phys. Fluids **27**, 1301 (1984) and references therein.
15. W. C. Mead, E. K. Stover, R. L. Kauffman et al., Phys. Rev. A**38**, 5275 (1988) and references therein.
16. P. D. Goldstone, S. R. Goldman, W. C. Mead et al., Phys. Rev. Lett. **59**, 56 (1987); P. D. Goldstone, private communication (1989).
17. R. A. Bosch, E. F. Gabl, J. D. Simpson et al., Bull. Am. Phys. Soc. **34**, 2113 (1989).

UNCLASSIFIED SECRET/RD

UNCLASSIFIED SECRET/RD

18. W. C. Mead, S. V. Coggeshall, and N. D. Delamater, "Conversion of Laser Light to X-Rays in Hohlraum Environments (U)," in *Proceedings of the 1986 Topical Conference on the Physics of Radiatively Driven ICF Targets* (U), edited by D. L. Cook, Sandia National Laboratories report SAND 87-0793 RS1260/87/4 (SRD) (1987), pp. 178–183.
19. M. Cray, W. C. Mead, and G. R. Magelssen, "Theoretical Study of an Important Aspect of Hohlraum Dynamics (U)," Los Alamos National Laboratory report X-1-90-074 (SRD) (1990); to be published in *Proceedings of JOWOG 37* (U), Sandia National Laboratories report, January 22-25 (SRD) (1990).
20. W. C. Mead, B. Bezzerides, S. R. Goldman, E. K. Stover, "KrF Laser-Driven Hohlraums (U)," Los Alamos National Laboratory report X-1-85-5 (SRD) (1985), and in *Proceedings of the 1984 Topical Conference on the Physics of Radiatively Driven ICF Targets* (U), Los Alamos National Laboratory report LA-CP-85-138 (SRD) (1985).
21. J. D. Lindl, private communication (1988); J. D. Lindl, "LMF Hohlraum Designs ... (U)," in *Target Physics Review* (U), Lawrence Livermore National Laboratory report CLYC 88-0023A (SRD) (1988), pp. 111ff; A. R. Thiessen, "Some Aspects of LMF Hohlraum Design (U)," in *Proceedings of the 1989 Topical Conference on the Physics of Radiatively Driven ICF Targets* (U), edited by E. M. Campbell and R. L. Kauffman, Lawrence Livermore National Laboratory report CLYE 89-0004 (SRD) (1989), pp. 455–468.
22. S. Haan, "Radiation Transport between Concentric Spheres (U)," Lawrence Livermore National Laboratory report COPD 83-64 (SRD) (1983).
23. W. C. Mead, "Intermediate Density Targets (U)," in *Laser Program Annual Report–1978*, Lawrence Livermore Laboratory report UCRL-50055-78, edited by M. J. Monsler (SRD) (1979), pp. 2–16 to 2–59; J. D. Lindl, "Hot Electron Scaling in Hohlraums ... (U)," in *Laser Program Annual Report–1980*, Lawrence Livermore National Laboratory report UCRL-50055-80, edited by L. W. Coleman and W. F. Krupke (SRD) (1981), pp. 2–2 to 2–8; W. L. Kruer, K. G. Estabrook, B. F. Lasinski, and A. B. Langdon, "Hot Electron Generation in Hohlraums (U)," loc. cit., pp. 2–39 to 2–43.
24. R. E. Turner, K. G. Estabrook, R. L. Kauffman et al., Phys. Rev. Lett. **54**, 189 (1985); R. P. Drake, private communication (1988–89).
25. M. D. Rosen, "Electron Transport and Preheat," in *Laser Program Annual Report–1979*, edited by L. W. Coleman, Lawrence Livermore National Laboratory report UCRL-50021-79 (1980), pp. 3–6 to 3–10; J. D. Lindl, "Tolerance of High-Gain ICF Capsules to Preheat by High-Energy Electrons (U)," in *Laser Program Annual Report–1984*, edited by M. L. Rufer and P. W. Murphy, Lawrence Livermore National Laboratory report UCRL-50055-84 (SRD) (1985), pp. 2–38 to 2–39.
26. B. F. Lasinski, private communication (1986).
27. R. D. Jones, W. C. Mead, S. V. Coggeshall, C. H. Aldrich et al., Phys. Fluids **31**, 1249 (1988), and references therein.
28. N. M. Hoffman and W. S. Varnum, private communication (1988–89).

UNCLASSIFIED
SECRET/RD